Under water Laser assisted ablation of alloyed Metal nanoparticles for surface plasmonic application

A THESIS

Submitted in partial fulfillment of the requirements for the award of the degree of

Master of Technology

in

Mechanical Engineering

with specialization in

Production and Industrial Engineering

by

Sanet Kumar Meena

(1502103011)

DISCIPLINE OF MECHANICAL ENGINEERING

INDIAN INSTITUTE OF TECHNOLOGY INDORE

JUNE 2017

INDIAN INSTITUTE OF TECHNOLOGY INDORE

CANDIDATE'S DECLARATION

I hereby certify that the work which is being presented in the M.Tech thesis entitled **"Under water Laser assisted ablation of alloyed Metal nanoparticles for surface plasmonic application"** in the partial fulfillment of the requirements for the award of the degree of **MASTER OFTECHNOLOGY** in **MECHANICALENGINEERING** with specialization in**PRODUCTIONandINDUSTRIALENGINEERING** and submitted in the**DISCIPLINE OF MECHANICAL ENGINEERING** at **INDIAN INSTITUTE OF TECHNOLOGY INDORE, INDIA**, is an authentic record of my own work carried outduring the time period from May 2016 to June 2017 under the supervision of **Dr. I. A.Palani** in Discipline of Mechanical Engineering and **Dr. Vipul Singh** in Discipline ofElectrical Engineering.

The matter presented in this thesis has not been submitted elsewhere by me for the award of any other degree.

Sanet Kumar Meena

This is to certify that the above statement made by the candidate is correct to the best of our knowledge.

Dr. I. A. Palani **Dr. Vipul Singh**

Sanet Kumar Meena has successfully passed his M.Tech. Oral Examination, held on............

Signature of M.Tech. Thesis Supervisors
Date:

Convener, DPGC
Date:

Signature of PSPC Member 1
Date:

Signature of PSPC Member 2
Date:

Signature of Chairman, Oral Examination Board with date

ACKNOWLEDGEMENT

There is lot of people whom I want to take this opportunity to thank for their valuable support in the course of my M.Tech project. My first and foremost gratitude goes to my supervisor, **Dr. I. A. Palani** for his honest and friendly guidance, his extremely useful ideas and endless support throughout the project. I thank him for his valuable time and immeasurable patience. My special thanks also go to my co-supervisor **Dr. Vipul Singh** for their excellent ideas and support. I am extremely thankful to all of my colleagues in the Production and Industrial Engineering in the Department of Mechanical Engineering at IIT Indore. I would also like to thank Ph.D. scholars of Opto-mechatronics and Instrumentation group, especially, **Mrs. Nandini Patra** for their useful constructive guidance, fruitful stimulating discussions and mutual support needed for the continuation of the M.Tech project. I am grateful to the Mechanical Engineering department and Sophisticated Instrumentation Centre (SIC) of IIT Indore for the financial and technical support to carry out the above investigations. I also express my gratitude towards Ms. Sonam Mandani, PhD scholar in Chemistry for her help with DLS measurements. Finally, I am extremely grateful to my family for their patience, compromise, continuous moral support and understanding during the last two years in which most of my time and energy was devoted to the completion of this project.

Sanet Kumar Meena

Dedicated to my Guide –

my father,

my grandfather,

my teacher,

and my friends

ABSTRACT

Liquid assisted laser ablation on a rotating target has become a key synthesis method for generating metal alloy nanoparticles with their controlled geometry and crystallinity. The laser ablation of metal targets in liquid environments is considered as a reliable alternative to traditional chemical reduction methods for obtaining metal colloids, since such a strategy is considered environmental friendly ("green" technique) with products which frequently do not need stabilizing molecules or other chemical precursor. Laser ablation-based synthesis can be executed in deionized water or even in biologically-compatible aqueous solutions like Acetone, Isopropyl alcohol, Ethanol etc.

On the other hand, metal nanoparticles are often susceptible to oxidation and aggregation (thus reducing their free energy), leading to a loss of their physical properties. Therefore, several efforts are taken to protect metal nanoparticles with inert shells, to preserve them from surface modifications and to keep their main characteristics unchanged.

In this M.Tech thesis we have synthesized Al, Cu-Al and NiTialloy nanoparticles with different laser fluences (30,40,50 J/cm^2), wavelengths (1064,532,355 nm), Rotational speeds (10,20,30 RPM) but with a constant flow rate of liquid medium. The main objective is to study morphology, crystallinity and optical propertyof these metal alloy nanoparticles for Suface Plasmonic application.

The Particles shape, surface morphology, size and crystallinity were analyzed through SEM, DLS and XRD characterizations respectively. UV-Vis is used to check the absorption of nanoparticles and thermal analysis of NiTi particles is done by DSC.

LIST OF PUBLICATIONS

Papers in Conference

- **Sanet K. Meena,** Nandini Patra, Vipul Singh, I. A. Palani "Investigations on Nd:YAG nanosecond liquid assisted laser ablation of rotating target towards the generation of spherical Al nanoparticles" (25^{th} DAE-BRNS National Laser Symposium).

Table of contents

List of figures

List of tables

Chapter 1 Introduction

1.1 Background

Nanoparticles are a new class of materials with unique properties[1]. Being in the size range of 1-100 nm, NPs have higher surface area than volume. This enormous surface area and associated electronic properties impart special character to NPs which are not found in their bulk counterparts[2]. For example, NPs have shown a size dependent optical tunability across the entire visible range[3]. In certain sizes, the collective oscillation of electrons known as surface plasmon resonance can be observed, which is quite different than in bulk materials[4]. Furthermore, NPs can be effective catalysts owing to their large surface area. They also show remarkable 2D self-assembly which could be very useful for making thin film devices[5]. These striking properties associated with NPs make them ideal candidates for various applications.

1.2 Plasmonic solar cell

A Plasmonic solar cell is a type of thin film solar cell that converts light into electricity with the assistance of plasmons[6]They are typically less than 2 μm thick and theoretically could be as thin as 100 nm[7]. They can use substrates which are cheaper than silicon, such as glass, plastic or steel. One of the challenges for thin film solar cells is that they do not absorb as much light as thicker solar cells made with materials with the same absorption coefficient. Methods for light trapping are important for thin film solar cells[8]. Plasmonic cells improve absorption by scattering light using metal nano-particles excited at their surface plasmon resonance[9] Incoming light at the plasmon resonance frequency induces electron oscillations at the surface of the nanoparticles. The oscillation electrons can then be captured by a conductive layer producing an electrical current. The voltage produced is dependent on the bandgap of the conductive layer and the potential of the electrolyte in contact with the nanoparticles. There is still considerable research necessary to enable the technology to reach its full potential and commercialization of plasmonic enhanced solar cells.

1.2.1 Localised Surface plasmon (LSP):

- Localised Surface plasmon (LSP) is indused when frequency of the oscillation excited electron of metallic particle is matched with the frequency of the incident photon.
- The local enhancemnt of the electromagnetic field as a result of the resonance effect leads to the effective light concentration near the surrounding of the metallic particle.

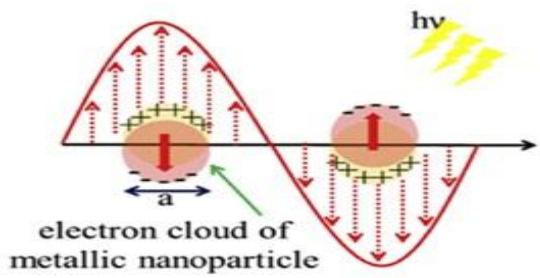

Figure 1 LSP confined in the spherical metallic nanoparticles

1.3 Nanoparticles

The field of nanotechnology is one of the most active research areas in modern materials science. Nanoparticles exhibit new or improved properties based on specific characteristics such as size, distribution and morphology.

There have been impressive developments in the field of nanotechnology in the recent past years, with numerous methodologies developed to synthesize nanoparticles of particular shape and size depending on specific requirements. New applications of nanoparticles and nanomaterials are increasing rapidly. Nanotechnology can be termed as the synthesis, characterization, exploration and application of nanosized (1-100nm) materials for the development of science. It deals with the materials whose structures exhibit significantly novel and improved physical, chemical, and biological properties, phenomena, and functionality due to their nano scaled size. Because of their size, nanoparticles have a larger surface area than macro-sized materials. The intrinsic properties of metal nanoparticles are mainly determined by size, shape, composition, crystallinity and morphology. Nanoparticles, because of their small size, have distinct properties compared to the bulk form of the same material, thus offering many new developments in the fields of biosensors, biomedicine, and bio nanotechnology. Nanotechnology is also being utilized in medicine for diagnosis, therapeutic drug delivery and the development of treatments for many diseases and disorders. Nanotechnology is an enormously powerful technology, which holds a huge promise for the design and development of many types of novel products with its potential medical applications on early disease detection, treatment, and prevention.

1.3.1 Methods of Nanoparticle Synthesis

Various techniques of nanoparticle is summarized in the following flow chart. Broadly it can be classified into two, i.e. Top-down method and Bottom-up method.

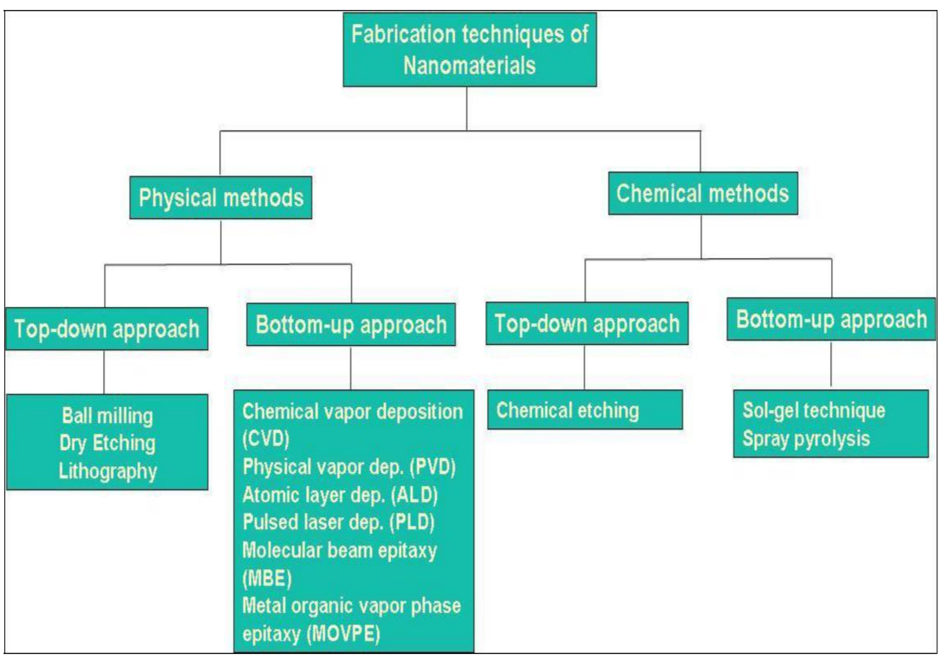

Figure 2 Flowchart shows fabrication techniques of nanomaterials.

The “top-down” approach involves the breaking down of large pieces of material to generate the required nanostructures from them. This method is particularly suitable for making interconnected and integrated structures such as in electronic circuitry.

In the "bottom-up" approach, single atoms and molecules are assembled into larger nanostructures. This is a very powerful method of creating identical structures with atomic precision, although to date, the man-made materials generated in this way are still much simpler than nature's complex structures.

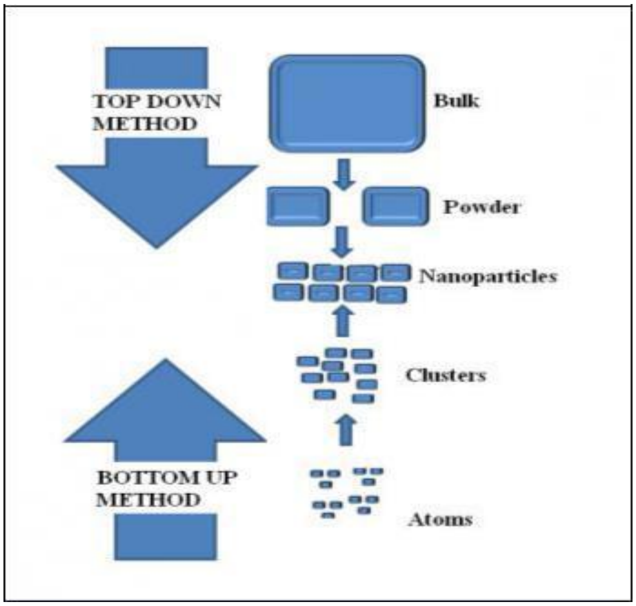

Figure 3 Bottom-up and Top-down approach

Althoughvarious techniques have been summarized, there are some features to consider that are common to all methods. That is, the synthesis of nanoparticles requires the use of a device or process that fulfills the following conditions:

- Control of particle size, size distribution, shape, crystal structure and composition distribution
- Improvement of the purity of nanoparticles (lower impurities)
- Control of aggregation
- Stabilization of physical properties, structures and reactants
- Higher reproducibility
- Higher mass production, scale-up and lower cost

1.2.2 Characteristics of Nanoparticles:

Nanomaterials have superior properties than bulk substances. Various characteristics of different nanoparticles relative to bulk metals are summarized below-

1. *Optical function*: The surface absorbing Plasmon of Au and Ag can express various colors by changing the size of the particle, the form or shape of the particle, and the rate of condensation. A new paint that has the durability of inorganic pigment and the vivid color of an organic substrate can be made.

Nanoparticles smaller than the wavelength of light can be used to make penetration conductivitymaterials (there is little absorption, dispersion and reflection).

2. *Catalyst function*: Reaction efficiency can be enhanced since the specific surfacearea of such nanoparticles is large compared with existing particles, to the extent that the surface terrace is regular at the atomic level, a hyperactive catalyst with high selectivity can be made, for example, Au nanoparticles.

3. *Thermal function*: when the particle diameter is small (less than 10 nm), themelting point is lower that a bulk metal. Electronic wiring can be made with nanoparticles that have low boiling point, like polymer.

4. *Electrical function*: Since superconductivity transition temperature rises so thatparticle diameter is small (less than 1 nm), it can be used to make high temperature superconductivity material.

5. *Mechanical function*: Since the mechanical characteristics improved, mechanicalstrength can be sharply raised by mixing the nanoparticles with metals or ceramics.

6. *Magnetic function*:

The attractive force of a magnetic metal increases onreduction of the particle diameter, such that soft-magnetic materials can be made in the form of an alloy of nanoparticles. Moreover, a permanent magnet can be made if the nanoparticles are smaller than the magnetic domain made to magnetize.

1.3 Why Al Nanoparticles:

Spherical Aluminum (Al) nanoparticles have potential application in the field of surface plasmon resonance as it has maximum surface to volume ratio. Thus the scattering through spheres are maximum which helps to improve the absorption of Plasmonic solar cell[10]. Al nanoparticles are significantly used in solar cell application due its high absorption at UV spectrum[4]. Physical and chemical properties make them suitable to use in different application of automobiles and aircrafts. These are heat shielding coatings, corrosion resistant, conductive and heat reflecting paints, conductive and decorative plastics, soldering and termite welding, pyrotechnics and military applications (rocket fuel, igniter, smokes, and tracers) to enhance the quality of respective field[2], [11].

It comprises a little over 8% of the earth's crust and third most common element after Oxygen and Silicon. Good thermal and electrical conductivity.

Biomaterial: Improved biocompatibility. It present in our body and Non-Toxic. Our body daily intake of Al is 10-110 mg.

Heat transfer fluids: Utilizing Nano fluid as an absorber fluid is an effective approach to enhance Heat transfer in solar devices. It reduces Solar Collector area about 21.5%.So, reduces weight, energy and cost to manufacturing.

1.4 Why Cu-Al Alloy Nanoparticles:

Table 1 Properties of Al and Cu.

Properties	Al	Cu
Boiling Point (ºC)	2519	2562
Melting Point (ºC)	660.32	1084.62
Density (g/cc)	2.7	8.96
Thermal Conductivity (W/m- ºC)	237	401
Absorbance range	Ultra-Violet	Visible

Absorptionof light of Al in Ultra-Violet range and Cu in Visible range. So there is the possibility in Cu-Al alloy that it absorb the light in both ranges. If it happenthan it is greatest advantage that we can use the Cu-Al nanoparticles in Plasmonic Solar cell.

1.5 Why (NiTi) Alloy Nanoparticles:

Nitinol or Nickel Titanium (also known as NiTi) is in the unique class of shapememory alloys. Nitinol shape memory alloys can be modified to a great extent bychanges in composition, mechanical working, and heat treatment. This alloy also exhibits the superelasticity or pseudoelasticity.

Nickel and titanium belongs to D block, period 4 elements. A major portion of mined nickel comes from laterite and magmatic sulfide ores. Titanium is found in igneous rocks and sediments derived from them. Nickel Titanium (NiTi) nanoparticles, nanodots, or nanopowder are black spherical high surface area alloy particles. Nanoscale Nickel Titanium particles are typically 10 – 40 nanometers (nm) with specific surface area (SSA) in the range of 30 - 50 m^2/g. Nano NiTi particles are also available in passivized form and ultra-high purity and coated dispersed forms. They are also available as a nanofluid through the AE nanofluid protection group.

Table 2 Some other properties of the NiTi alloys are listed (9)

Properties	Nitinol (martensite (M)/austenite (A))
Melting Point (ºC)	1310
Density (g/cc)	6.5
Electrical Resistivity (μΩ-cm)	76 (M) / 82 (A)
Thermal Expansion (10-6/ ºC)	6.6 (M) / 11 (A)
Thermal Conductivity (W/m- ºC)	18
Elastic Modulus (GPa)	40 (M) / 75 (A)

<u>Medical Uses</u>:

- Nitinol stents are another significant application of this metal in medicines.
- Its biocompatible properties make useful in orthopedic implants.
- Nitinol wires can be used for marking and locating breast tumors.
- Dentistry

Industrial Uses:

- This metal is often used in mechanical watch springs.
- Nitinol spring is used in various industries for the purpose of utilizing the super elastic properties of this metal.
- It is a popular choice for making extremely resilient glass-frames.
- The replacement of platinum with nickel titanium nanoparticles in automotive catalytic converters would significantly reduce their cost.
- Catalytic functions such as in the anode of solid oxide fuel cells.
- In coatings, plastics, nanowires, nanofibers, and textiles.

1.6 Laser Ablation:

Laser ablation is the process of removing material from a solid (or occasionally liquid) surface by irradiating it with a laser beam. Usually a pulsed laser is used for removing the material but it is also possible to ablate material with a continuous wave laser beam if the laser intensity is high enough. Short pulse laser ablation is advantageous since the material can be heated up to temperature of vaporization in a very short time [12]. This means that the energy does not have time to spread into the deeper parts of the material and thereby the energy is localized where it is needed. Pulsed lasers can be classified as nanosecond, picosecond or femtosecond lasers based on the duration of laser pulse. The depth over which the laser is absorbed and thus the amount of material removed by a single laser pulse depends on the material's optical properties,the laser wavelength and the pulse length[13]

Laser ablation can be carried out in conventional deposition chamber with vacuum or filled gas and also in liquids. Laser ablation in liquids has been intensely pursued in recent decades because of its enormous potential for technological applications such as high temperature chemical synthesis and laser based material processing [13]. Laser ablation in liquids is divided into categories, the laser ablation of the solid at the gas-liquid interface or at the liquid-solid interface. Laser ablation in liquids has a great potential for medical applications when laser irradiation is guarded inside the human body to ablate soft tissues [14]. Laser ablation of a solid target in confined liquids is also very useful in the synthesis of nanostructures in a chemically inert environment.

1.6.1 Principle of Laser Ablation:

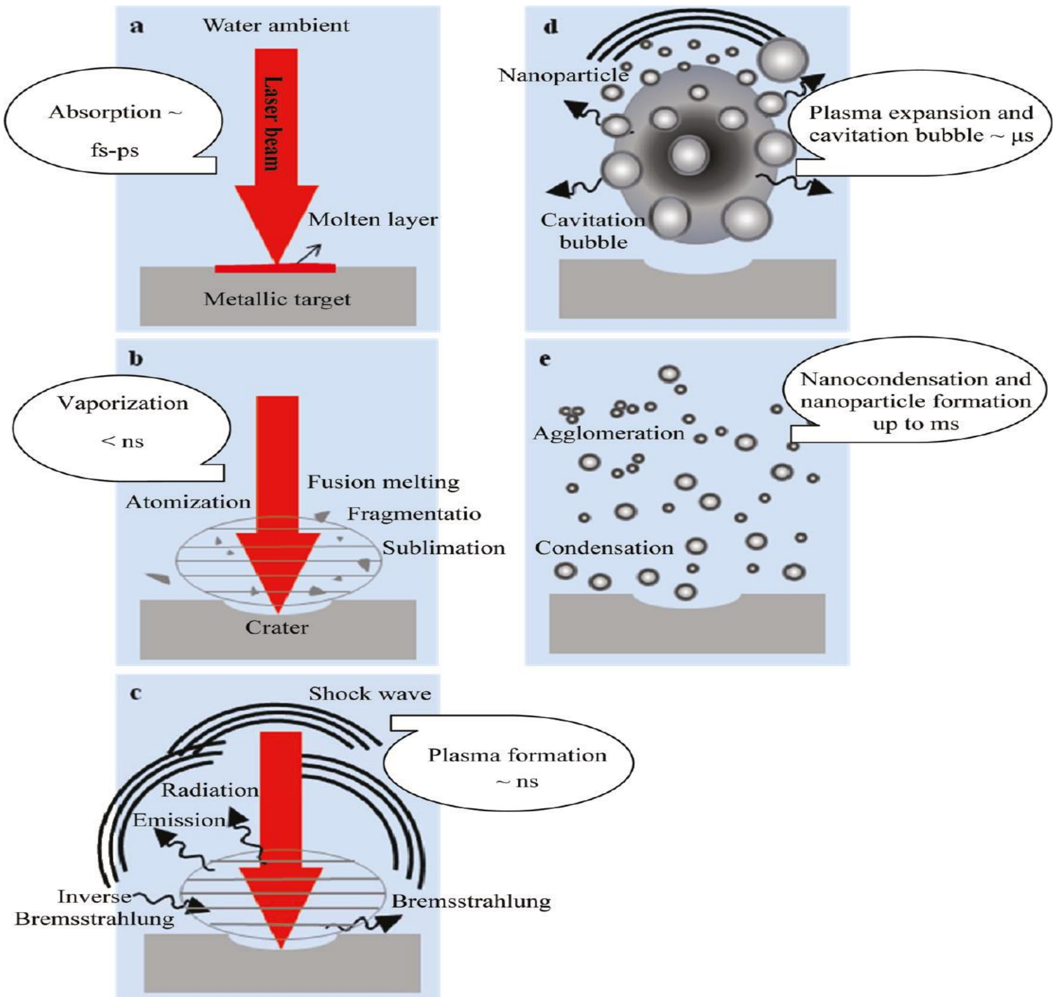

Figure 4 Sequential steps for nanoparticle generation using nanosecond laser in water: (a) laser absorption (fs-ps interval), (b) vaporization (less than ns), (c) plasma formation (during ns), (d) plasma expansion and cavitation bubble (during μs), and (e) nanoparticle formation (up to ms)[15].

Here a pulsed laser beam is focused on a target in a solvent and the solid target absorbs the laser pulse energy. Different routes are available for ablation to occur, viz. spallation (ejection of fragments of material following the passage of a tensile stress wave), phase explosion (decomposition of a thermodynamically metastable homogeneous liquid into a mixture of liquid droplets and gas), fragmentation (disintegration of a homogeneous material into clusters under the action of large strain rates) and vaporization (passage from the solid or liquid to the gas phase), asa function of increasing fluence. In simple language it can be stated that three main steps contribute in laser ablation synthesis method and formation of nanoparticles from a target immersed in liquid. Laser pulse, first, heats up the target surface to the boiling point, and thus, plasma plume containing vapor atoms of target is generated. Then, plasma expands adiabatically; and finally, nanoparticles will be generated when condensation occurs. Synthesis parameters such as laser wavelength, laser energy, pulse width, liquid media type, and ablation time can notably affect the product characteristics.

When the laser fluence exceeds the ablation threshold value for the material, chemical bonds are broken and the material is fractured into energetic fragments.

1.6.2 Analysis of Generated Plume:

The plume generated on the target submerged in water is confined to a small region by the pressure of water and shows extremely high pressure of the order of a few GPa in the initial stage. Because the temperature in the vapor plume can rise to high values (10,000 K and higher), a plasma will be formed. Since the material leaves the reaction zone as energetic plasma, gas and solids debris mixture, the ablation process resembles explosive evaporation of the material. Hence, the vapor plume does not only consist of atoms, but also of electrons and ions. Besides atoms, electrons and ions, the material plume also consists of particles, with dimensions ranging from nanometer till micrometer. Because of the formation of plasma in front of the target, the laser beam will be partially absorbed before it reaches the target, i.e. so called 'plasma shielding'. Laser radiation is absorbed primarily by inverse Bremsstrahlung, which involves the absorption of a photon by a free electron. The plasma plume thus created expands and condenses in the liquid, forming a colloidal solution of nanoparticles. A unique property of the ablation process is that most of the absorbed energy is deposited in the ejected material, so that there is little or no thermal damage to the surrounding target material.

1.6.3 Operating Parameters for Laser Ablation:

Table 3 Operating parameters for laser ablation

S. No.	Operating parameter	Range
1	Wavelength of Laser Beam	UV [200-400 nm] Visible [400-800 nm] IR [800 nm-1 μm]
2	Laser Fluence	1-100 J/cm^2
3	Pulse Length	Nanosecond [10^{-9} seconds] Picoseconds [10^{-12} seconds] Femtosecond [10^{-15} seconds]
4	Target Material	Metals Alloys Organic Solids Semiconductors
5	Environment	Liquid Environment [Water, Acetone] Gaseous Environment [Ar, Ne] Vacuum

Modification of the size, shape, phase, morphology, and composition of the nanomaterials produced can be achieved through the adjustment of laser processing parameters, which is crucial for improving the performance and hence application of nanomaterials. If a structure on the tens of micrometers scale is the aim of the applications then nanosecond laser will often provide sufficient accuracy and will typically have a greater throughput, thereby making it apreferred solution.

If however, a feature of the nanometer scale is required, a pico- or femtosecond laser would be a better choice.

1.6.4 Laser ablation of solids in liquid environments

The most important difference between laser ablation of solids in vacuum or diluted gas and in liquids is that liquids confine the movement of the plasma plume. Therefore, a series of processes including generation, transformation, and condensation of the plasma plume resulting from laser ablation of solids in liquid environments takes place under the condition of the liquid confinement. Importantly, the confinement from liquids can greatly influence the thermodynamic and kinetic properties of the evolution of the plasma plume, and further causedistinctly the different environments of the condensing phase formation from that of laser ablation of solids in vacuum or diluted gas. Therefore, the understanding of fundamental aspects of the evolution of the plasma plume from laser ablation of solids in liquids is essential to find important potential in technology such as materials processing.

Chapter 2 Literature Review and Research objective

2.1 Past work on enhancement efficiency of solar cell using SPR:

S. Pillai et.al 2007[7]In this article they investigated the suitability of localizedsurface plasmons on silver nanoparticles for enhancing the absorbance of silicon solar cells. They findthat surface plasmons can increase the spectral response of thin-film cells over almost the entiresolar spectrum. At wavelengths close to the band gap of Si they observed a significant enhancement ofthe absorption for both thin-film and wafer-based structures. They reported a sevenfold enhancement forwafer-based cells at λ=1200 nm and up to 16-fold enhancement at λ =1050 nm for 1.25 μm thinsilicon-on-insulator (SOI) cells, and compare the results with a theoretical dipole-waveguide model.They also reported a close to 12-fold enhancement in the electroluminescence from ultrathin SOIlight-emitting diodes and investigate the effect of varying the particle size on that enhancement.

D. Zhang et.al 2014[4]In this paper, the surface plasmon resonance-enhanced optical absorption in thin silicon solar cells through aluminum sphere nanoparticles (NPs) was investigated. The effect of particle size and the distance between particles on absorption enhancement is studied using a finite-difference time-domain technique. The results showed that an enhancement of 40 % in absorption could be achieved by integrating the aluminum particles on thin silicon solar cells with the proper combination of NP parameters compared to those without aluminum particles.

2.2 Past Work using NiTi Alloy Target

Barcikowski et.al 2010 [16] generated NiTi NPs by a femtosecond laser system.They characterized the material properties and the phase transformation of the NPs by differential scanning calorimetry (DSC) and demonstrated the phase transformation of the laser-generated NPs. In this case, the aim was to deposit the NPs onto an implant surface and to determine their biocompatibility by incubation of human adipose derived stem cells with NiTi NPs.

M. Chakif et.al 2014 [17] investigated as a model system for a binary alloywhere the properties strongly depend on the relative proportion of the two elements and on the grain size. The NiTi nanoparticles were generated by laser ablation in water and used transmission electron microscopy (TEM) and dynamic light scattering (DLS), found a broad particle size distribution (10-200 nm). This effect could be caused by a change of the generated NPs by the laser irradiation again after the ablation, leading to coalesce and maybe fracture.

Mohammad Hossein Mahdieh et.al 2015 [18] used pulsed laserablation method for synthesis of colloidal nanoparticles of aluminum and titaniumtargets in distilled water, ethanol, and acetone as liquid environments. Ultraviolet– visible (UV–vis) absorption spectrophotometer and scanning electron microscope (SEM) were used for characterization of produced nanoparticles. Using image processing technique and analyzing the SEM images, nanoparticles mean size and size distribution were achieved.

2.3 Past work on solution assisted laser ablation

Nguyen The Binh et.al 2008[19]They studied to prepare silver nanoparticles by laser ablation. The characteristic spectral feature of the silver nanoparticles (peak around 400nm) was found in the absorption spectra measured by a UV-Vis 2450 spectrometer. The size and shape distribution of silver nanoparticles was observed and analyzed by a transmission electron microscope (JEM 1010- JEOL). Two different surfactants were employed namely trisodium citrate dihydrat $C_6H_7Na_3O_7$ and polyvinyl alcohol $(-CH_2-CHOH-)_n$. The size distribution and the UV-Vis absorption spectra of silver nanoparticles depend clearly on the properties and concentration of the surfactant employed. The experimental results were in good agreement with theory and showed advantages of the laser ablation method.

A. BALADI2012[11]Aluminum nanoparticles were synthesized by pulsed laser ablation of aluminum target inethanol, and this media prevented them from oxidation. Effect of laser wavelength wasstudied using 1064 and 533 nm wavelengths of a Nd:YAG laser with exerted energy of320 mJ/Pulse in 10 minutes. The results indicate that higher laser wavelength results inhigher ablation efficiency and finer spherical nanoparticles. Majority of nanoparticles inall samples are smaller than 100 nm, most of which are around 40-50 nm.

To study the effect of ablation time, laser ablation was carried out for 5, 10, and 15minutes in constant conditions (λ=1064 nm, E=280 mJ/pulse, in ethanol). It was seen thathigher ablation times resulted in more ablated mass and lower ablation rate. Absorptionof laser energy by primarily synthesized nanoparticles may be responsible for efficiencyreduction in higher ablation times (10-15 minutes), which also leads to occurrence offragmentation and size reduction of nanoparticles to about 33 nm.

David Omar Oseguera Galindo et.al 2016[20]The fundamental emission of a Nd:YAG laser (1064 nm), with an energy 0.1 J/pulse and a repetition rate of 10 Hz was employed to synthesize silver nanoparticles by ablation method confined in methanol and ethanol. The experimental setup allows synthesizing materials immersed in flammable solvents using an Argon atmosphere to prevent combustion, making the process safer when high fluence and high repetition rates of laser pulses are used. Transmission electron micrographs were taken for methanol and ethanol samples. The analysis of the methanol sample the day of synthesis and one month later, show that nanoparticles obtained were more dispersed, corresponding to better suspension stability. On the contrary, the images of nanoparticles in ethanol show a strong agglomeration, resulting in a fast sedimentation and less stability.

2.4 Identified Research Gaps:

From the literature review it can be concluded that

1. Limited Work has been done to investigate the influence of both Wavelength and Fluence together on the size, shape of nanoparticles in ablating the NiTi as a target material using Liquid Assisted Laser Processing.
2. Limited Work has been done to investigate the influence of both Wavelength and Fluence together on the size, shape of nanoparticles in ablating the NiTi as a target material using Liquid Assisted Laser Processing.
3. No work has been done to check the solution assisted laser ablation of Cu-Al alloy.

2.5 Objectives of the Present Research Work

a) Generate pure and stable nanoparticle of Al, Cu-Al and NiTi for further use as surface plasmonics (solar cells, photo-voltaic) to increase the absorption efficiency.

b) Study the nature of the generated nanoparticles in the shape, size and morphological behavior and also the effect of the laser parameters to these.

c) Check ablation rate in flowing liquid with different parameters.

d) Check the effect of solution on nanoparticles and find out good solution which avoid or reduce oxidation and aggregation of nanoparticles.

Chapter 3 Planning of Experiments and Techniques

3.1 Planning of the Experiments:

We planned the experiment to generate the alloyed metal nanoparticles according to the following:

i. Ablation of liquid assisted Al nanoparticles while laser irradiation on the periphery of the rotating target.

ii. Ablation of solution assisted Cu-Al nanoparticles while laser irradiation on the surface of rotating target.

iii. Ablation of liquid assisted NiTi nanoparticles while laser irradiation on the periphery of rotating target.

3.2 Experimental Procedure for Al nanoparticles ablation:

Experimental setup of nanoparticle generation is shown in Fig. 1 where the Nd:YAG nanosecond pulsed laser with a frequency of 10 Hz and pulse duration of 5–8 ns were used to ablate the Al target. Three different laser wavelengths of 1064 nm , 532 nm and 355 nm with two different fluences of 50J/cm^2 and 40 J/cm^2 were used to synthesize the Al nanoparticles where the target (Al 99.9%; Diameter 30 mm and height 6 mm) was rotating with a constant rotation speed of 10 r. p. m. The laser beam was focused on the circumference on the cylindrical target with a converging lens (f=50 cm) where the beam spot diameter of 0.5 mm was measured with the help of laser burn paper. A continuous flow of deionized water was applied at the focusing point of the target to ensure that the ablation should happen in liquid environment. The thickness of water layer above the target was around 3 mm and the ablation was happened for 10 minutes (6000 pulses). The nanoparticles generated by laser ablation were collected on a glass slide by evaporating the DI water on a hotplate. The particles shape, size distribution and phase transformation were analyzed by SEM, DLS and XRD respectively. Elemental analysis and Absorption capacities were investigated by EDAX (Energy Dispersive X-Ray Spectroscopy) and UV-Vis (Varian Cary 100) spectrum, respectively.

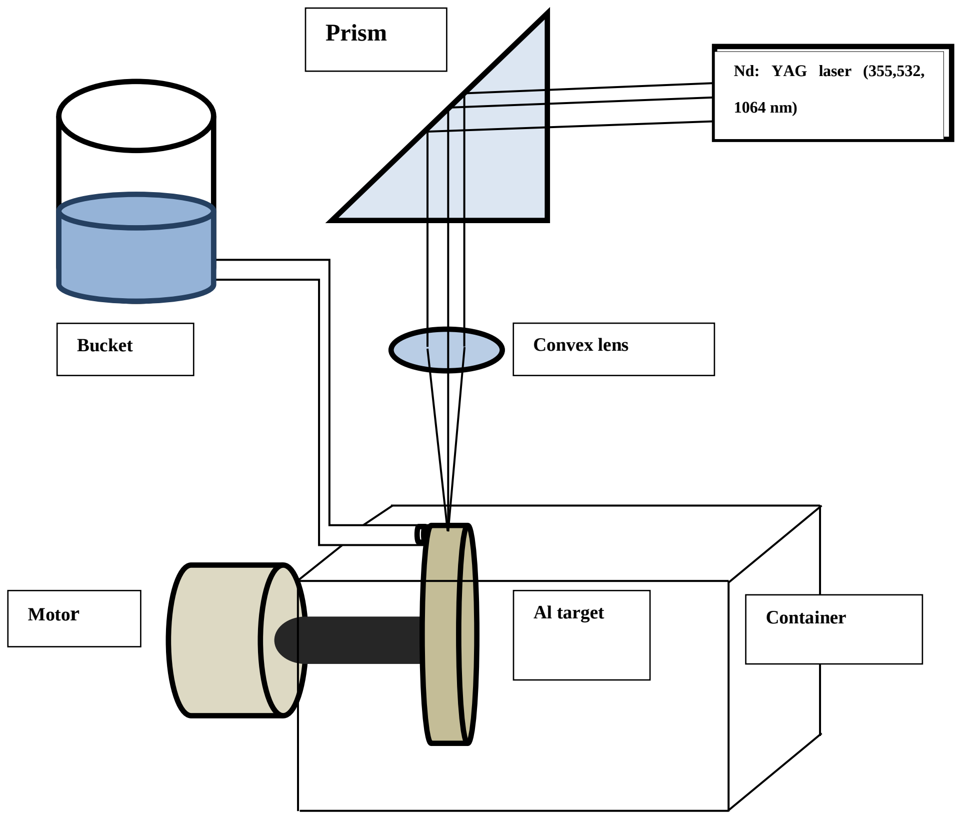

Figure 5 Schematic of the experimental setup for Al nanoparticles.

3.3 Experimental Procedure for NiTi nanoparticles ablation:

The below experiment setup used to synthesis the nanoparticle from the cylindrical NiTi target (dia: 30 mm and height: 6 mm) at 355 nm laser wavelength.The target (Nitinol 55 : 55% Ni and 45% Ti) was rotating at three different speed (10,20 and 30 RPM) for different laserfluences 30 J/cm^2, 40 J/cm^{2}and 50 J/cm^2. For each experiment ablation period was 15 min. All above characterization done for ablated Ni-Ti NPs in addition the DSC to check the thermal behavior of NPs.

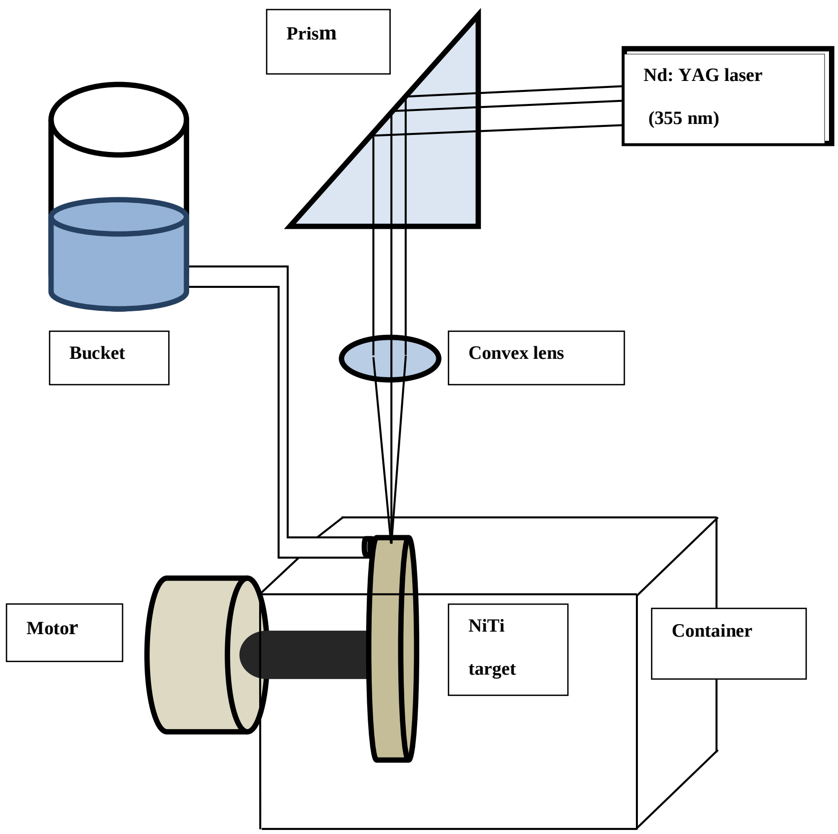

Figure 6 Experimental setup for Ni-Ti NPs.

3.4 Experimental Procedure for Cu-Al:

Figure 3 shows the layout of experimental setup. The Cu-Al (Cu 55% and Al 45%) nanoparticles were generated using Cu-Al target (dia: 30 mm and height: 6 mm) at 532 nm laser wavelength with two different Fluences40 J/cm^{2}and 50 J/cm^2. The target was placed in beaker and filled with 20 ml solution. The beaker put on XY-stage and given programming to rotate it at constant 10

RPM.Thesolution was made by using different solvent like Methanol, Ethanol, Acetone and IPA (Isopropyl alcohol) in different ratios with DI water.Surfactanttrisodium citrate dihydrat C6H7Na3O7 (SCD) also used with different concentration.

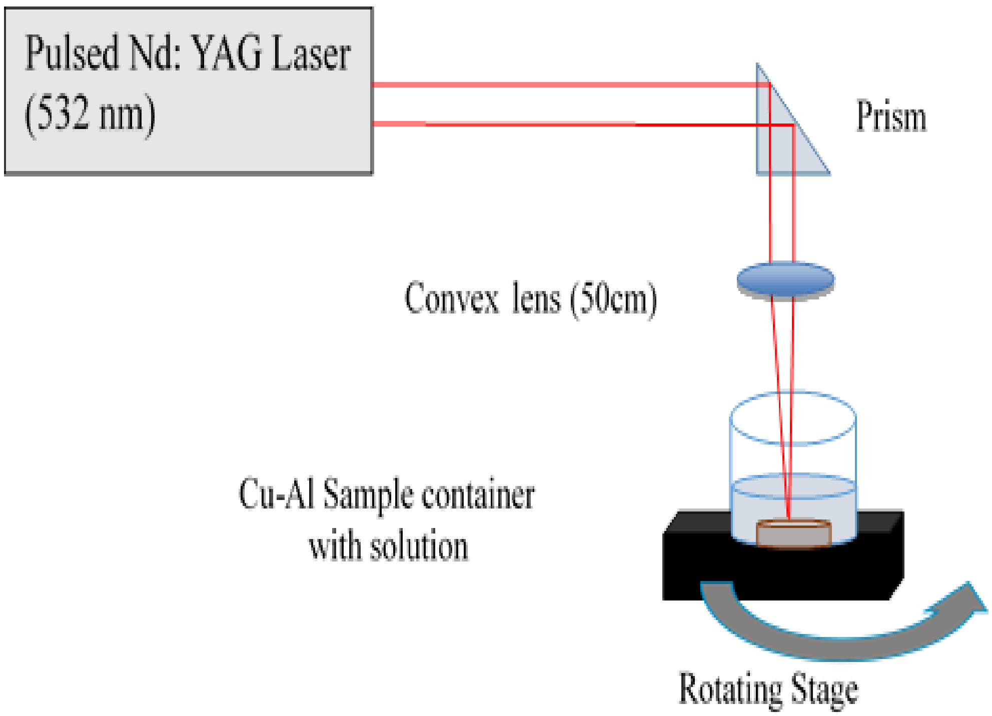

Figure 7 Experimental technique for Cu-Al NPs

3.5 Design of Experiments with Different Parameters:

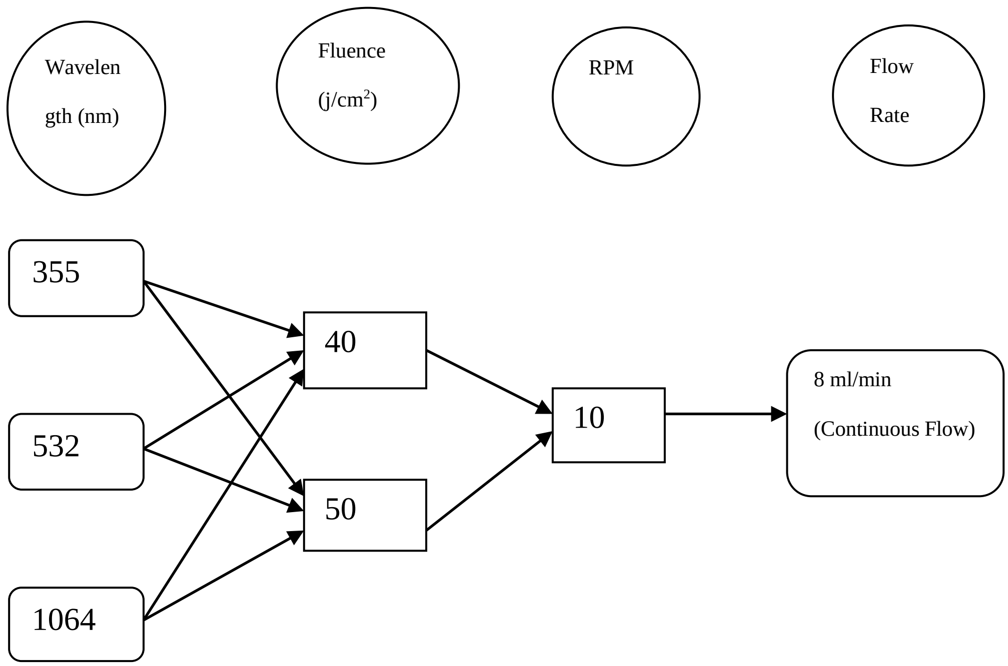

Figure 8 Flowchart shows the design of experiment for Al NPs

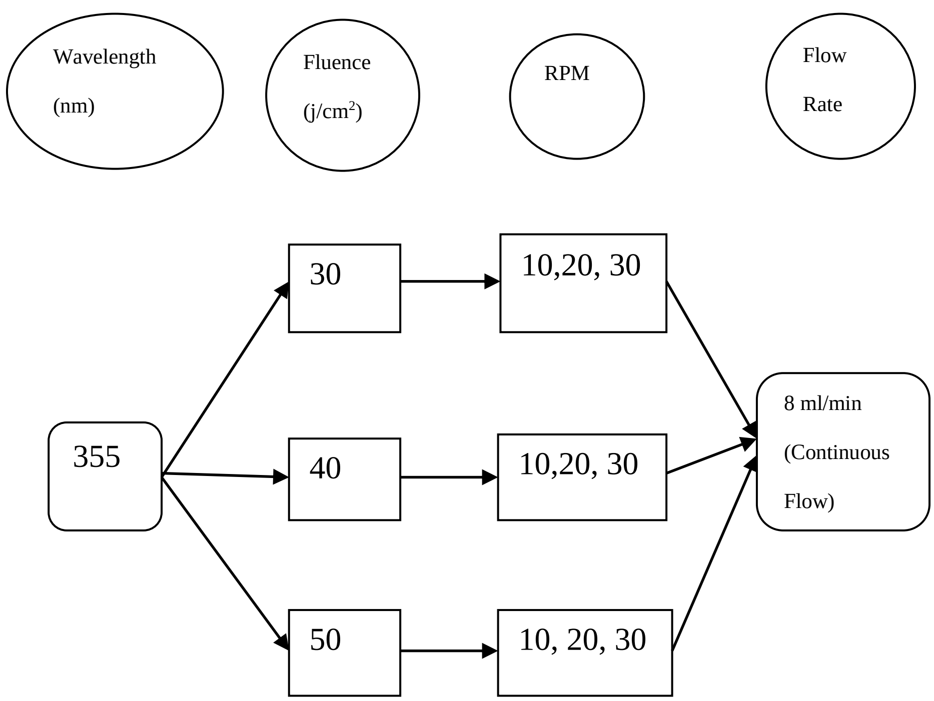

Figure 9 Flowchart shows the design of experiment for NiTi NPs.

Chapter 4 Results and Discussion

This chapter presents results of the experiments done with the rotating alloyed metal targets, their analysis (as characterization results) in variation of laser parameters and rotating speed.

4.1 Al Target:

The investigations on particle shape, surface morphology, size and crystallinity at three different laser wavelengths (1064 nm, 532 nm and 355 nm) with two different laser fluences (50 J/cm^2 and 40 J/cm^2) with constant rotational speed and flow rate are discussed in the following sections.

Table 4 Values of input parameters and Output values for different experiments

	Input Parameters			Output
Exp. No.	Wavelength (nm)	RPM	Fluence (J/cm^2)	Avg. Size (nm)
1	1064	10	40	214
2	1064	10	50	200
3	532	10	40	193
4	532	10	50	181
5	355	10	40	164
6	355	10	50	140

1 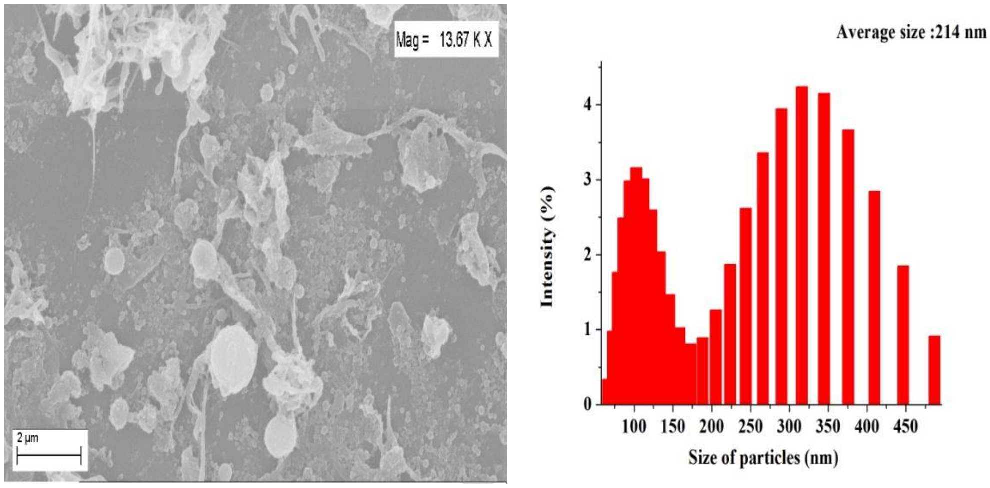
Mag = 13.67 K X
2 µm
Average size :214 nm
Intensity (%)
Size of particles (nm)
0
1
2
3
4
100 150 200 250 300 350 400 450

2 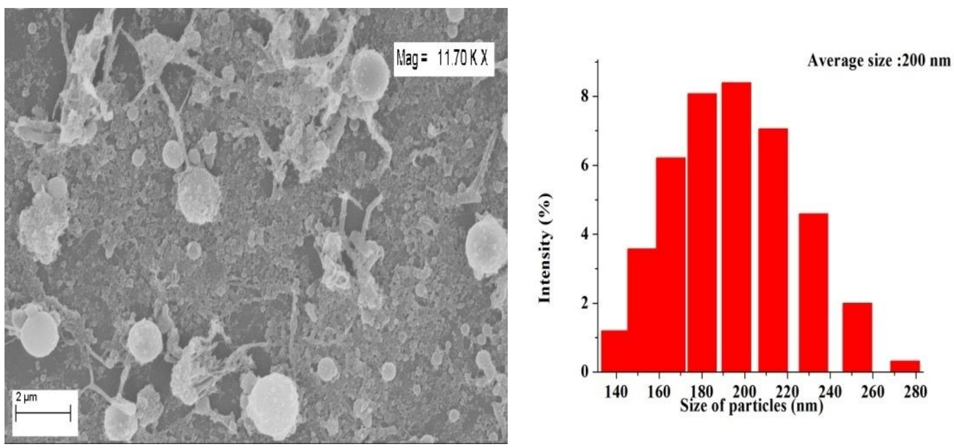
Mag = 11.70 K X
2 µm
Average size :200 nm
Intensity (%)
Size of particles (nm)
0
2
4
6
8
140 160 180 200 220 240 260 280

3 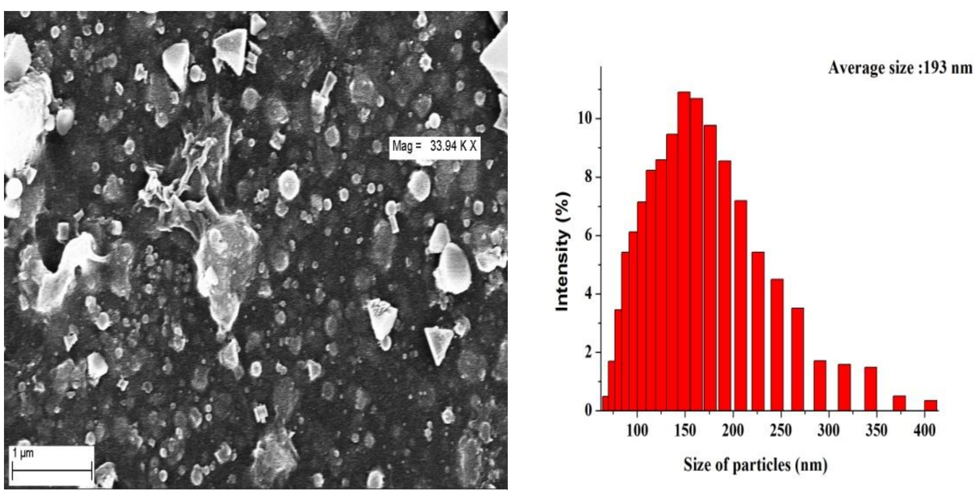
Mag = 33.94 K X
1 µm
Average size :193 nm
Intensity (%)
Size of particles (nm)
0
2
4
6
8
10
100 150 200 250 300 350 400

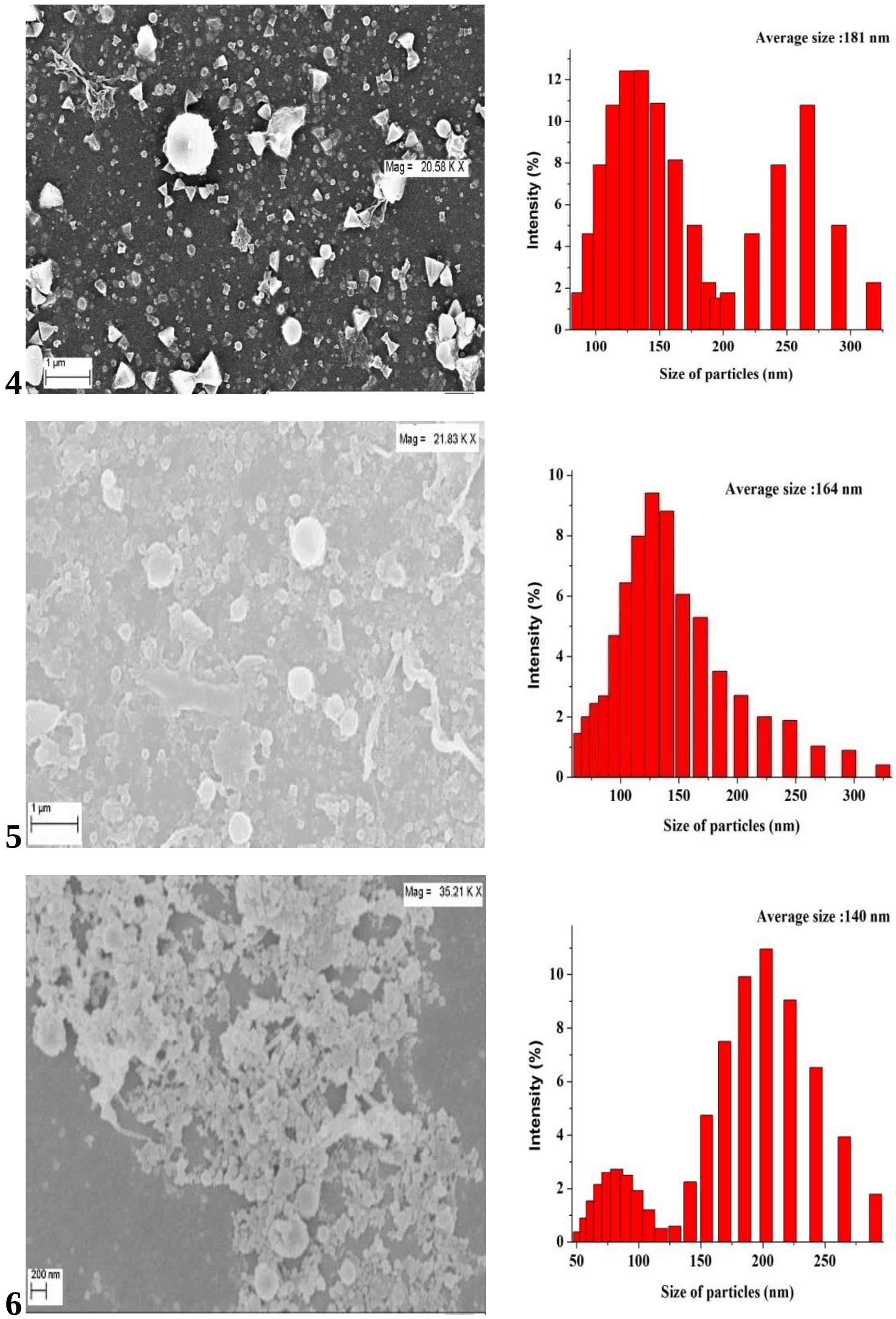

Figure 10 SEM Images and corresponding DLS plots(1-6) for different parameters as mention in table.

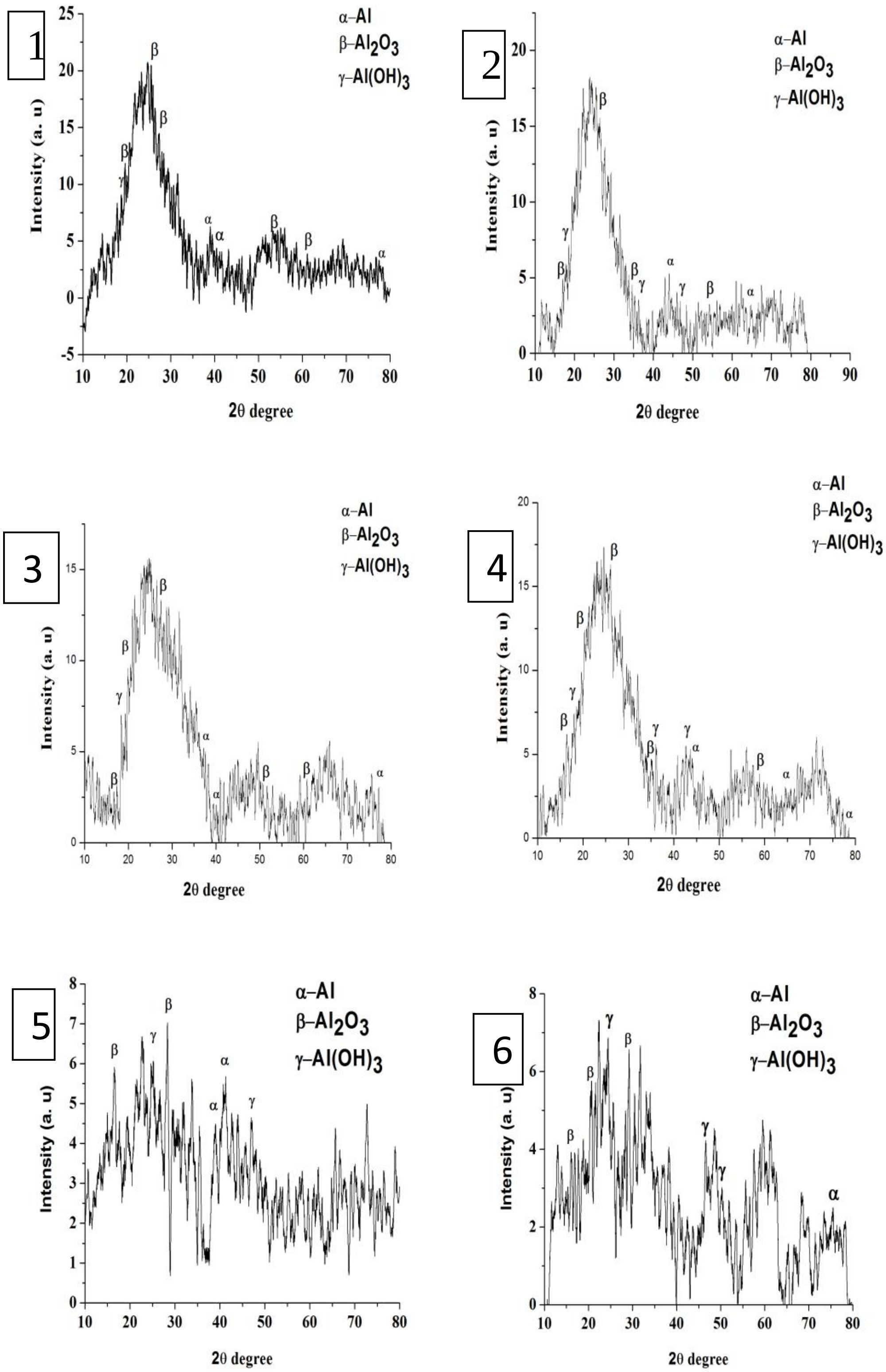

Figure 11 XRD plots (1-6) ofAlnanoparticles for the Different parameters as mention in table

4.1.1 Effect of laser wavelength and fluence:

Figure 10-12 shows the SEM, DLS, XRD and EDS analysis of Al nanoparticlesforthree different laser wavelengths (1064 nm, 532 nm and 355 nm) with two differentfluences (50 J/cm^2 and 40 J/cm^2). Spherical shape of nanoparticles were investigated (figure 10) where average particle size decrease with decrease in laser wavelength (table 4) and at constant wavelength average particle size decrease with increase in fluence (Table 4). The size of nanoparticle appears bigger in the SEM images which might be due to the aggregation of particles whereas DLS shows smaller average size of particles as the measurements were taken after the sonication and filtration of the samples which might help to break the aggregation of particles. It was observed that average particle size was smaller at 50 J/cm^2 than 40 J/cm^{2}fluence (Table 4). The possible reason might be due to the higher laser fluence leads to generate smaller size of nanoparticles. At high laser fluence, the temperature gradient inside the target material may be increased. Thus the colling rate of the material is also increased which leads to generate smaller size of particles[21]. The crystalline formation of Al nanoparticles were observed from the XRD images (figure 11) for three different laser wavelength and two different laser fluences (50 J/cm^2 and 40 J/cm^2). The peaks of pure Al, Al_2O_3 and Al $(OH)_3$ were observed[21] and indexed based on JCPDS-ICDD (Joint Committee on Powder Diffraction Standard-International Center for Diffraction Data) data card. The oxidations of Al nanoparticles were observed which might be due to the high oxidation potential of Al nanoparticles and the environment of ablation.

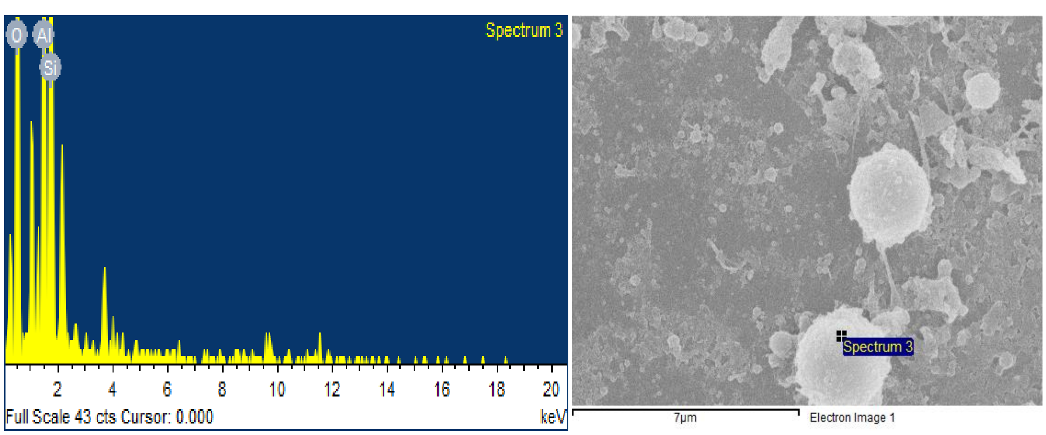

Figure 12 Elemental analysis of Al nanoparticles using EDS

4.1.2 Absorption spectra of Al nanoparticles:

Figure 13 shows the absorption spectra of as synthesized Al nanoparticles. It was observed that Al nanoparticles have higher absorption at UV range which might be due to the higher absorption of bulk Al metal at UV spectrum. Higher absorption of photons energy creates local thermal heating of the target material due to thermal conductivity of the material. This leads to melting, vaporization, plasma formation and finally particle ejection from the target material. In figure 13 it also observed that absorbance at fluence 50 J/cm^2 was much higher than 40 J/cm^{2}fluence for 532 nm and 355 nm wavelength. Absorbance was observed highest for 355 nm laser wavelength with fluence 50 J/cm^2 ablated nanoparticles.

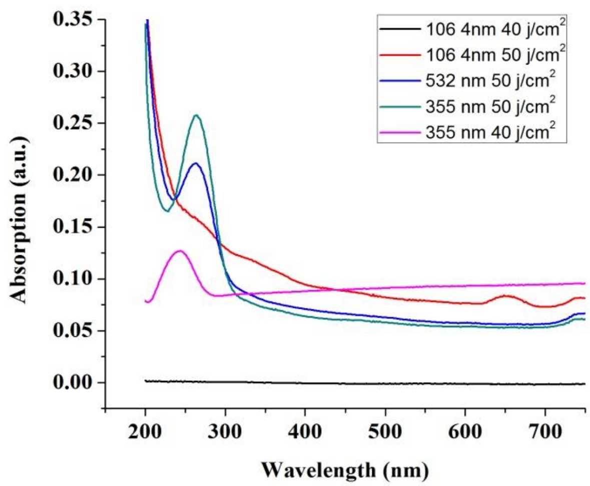

Figure 13 Absorption spectra of Al NPs corresponding to different parameters

4.2 Cu-Al Alloy Target:

The investigations on particle shape, surface morphology, size, crystallinity and stability at 532 nm laser wavelength with two different laser fluences (50 J/cm^2 and 40 J/cm^2) with constant rotational speed and in two different solution (IPA and Surfactant) is discussed in the following sections.

4.2.1 Cu-Al alloy nanoparticles in IPA solution:

First tests were performed in order to probe the instrumental setup. First we take solution 1:2 (IPA: DI Water) ratio of quantity. During ablation of NPs flame of

IPA combustion appear most of the times but when we take the solution in 1:4 ratios of quantities than no flame appear of IPA combustion and nanoparticles generated at 50 J/cm^2 and 40 J/cm^2 laser fluencies. Similarly test was performed in Methanol, Ethanol and Acetone solutions. It was investigated that in Acetone solution nanoparticles having smaller size distribution and longer dispersion. This may be due to higher dipole moment of Acetone reducing aggregation.

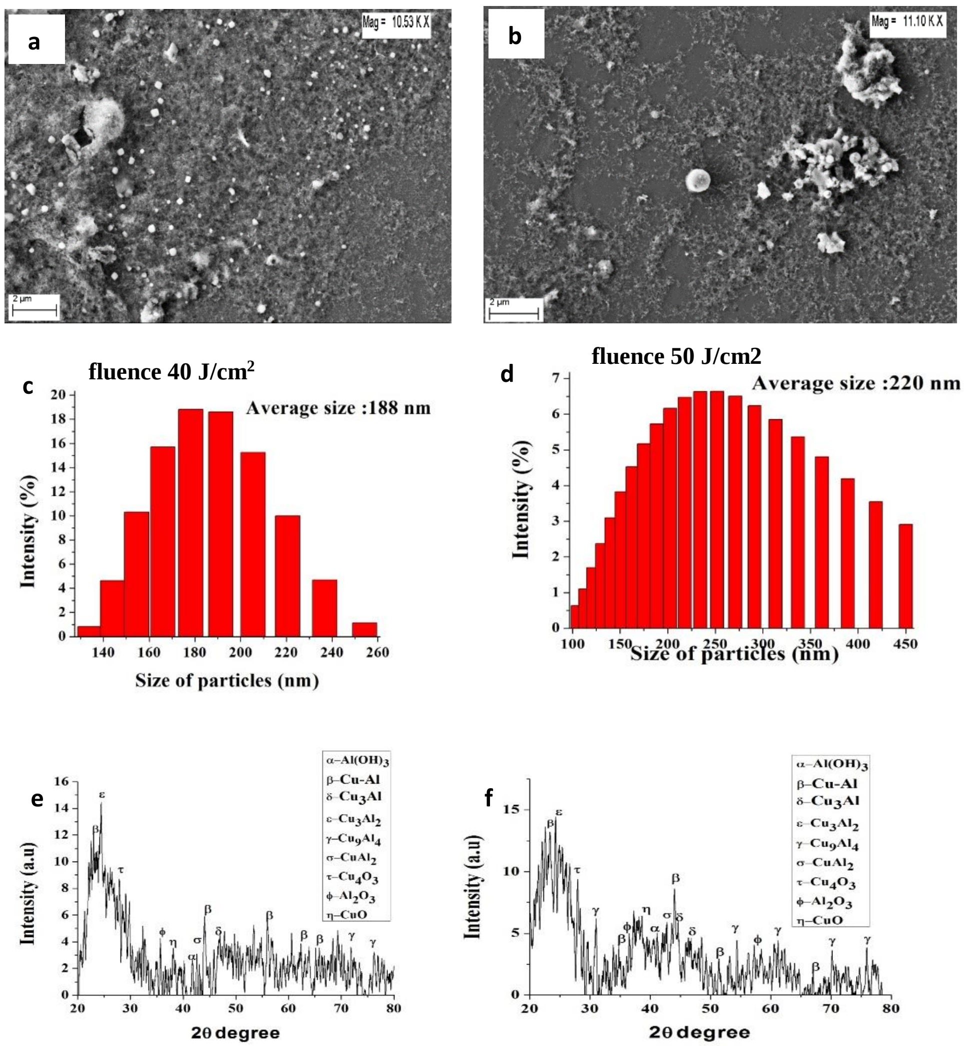

Figure 14 SEM (a, b) Images, DLS (c, d) Plots and XRD graphs corresponding to 50 j/cm2 and 40 j/cm2.

4.2.2 Cu-Al alloy nanoparticles in Surfactant solution:

We ablate the nanoparticles in tri-sodium Citrate Dihydrate (SCD) solution with three different concentrations (0.003M, 0.006M and 0.012M). It was observed that at 0.003M concentration better results obtained (figure 15). Nanoparticles ablated in this solution showing less aggregation figure 15(a, b) and lesser size distribution range figure 15(c, d). It may be due to surfactant modulates the available surface energy of the particles so that the surface tension decreases, and the Kelvin barrier moves, allowing more particles to escape the aggregation process and generally lowering the mean particle size.

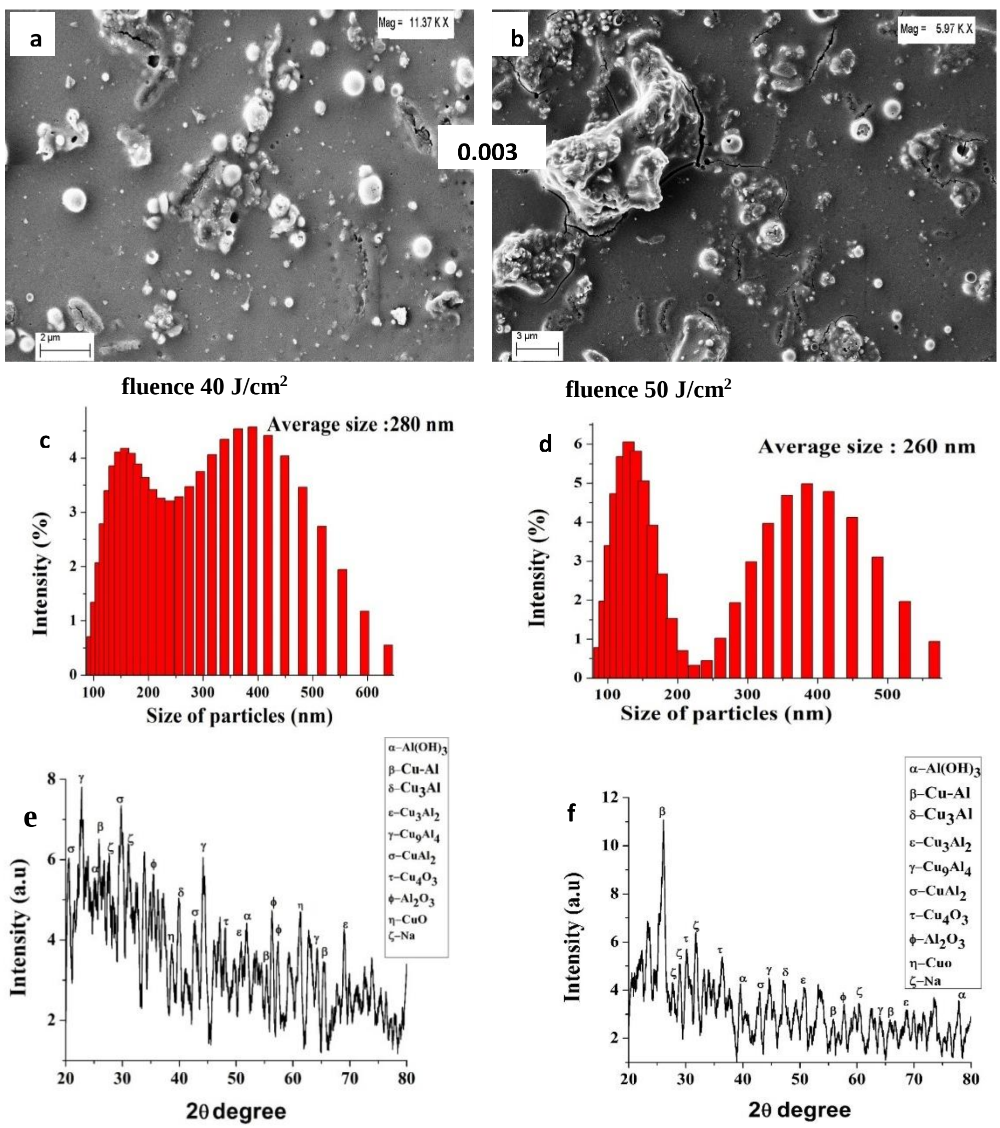

Figure 15 SEM (a, b) Images, DLS (c, d) Plots and XRD graphs corresponding to 50 j/cm2 and 40 j/cm2.

4.3 NiTialloy Target

4.3.1 Investigations on influence of 355 nm laser wavelength:

The investigation was done at a wavelength of 355 nm and with corresponding constant 10 RPM in figure 16 (1-3). The average particle size of 212 nm (Figure) was observed at laser fluence of 30 J/cm^2. Increasing the laser fluence to 40 J/cm^2, an average particle size of 190 nm (Figure) were observed. Further increase the laser fluence to 50 J/cm^2, an average particle size of 175 nm (Figure) was observed. Same can be observed at 20 RPM and 30 RPM in the figure 16 (4-6 and 7-9). Based on the above analysis, the average size has been tabulated in Table 5 where the effect of different values of laser fluence and different RPM on average size of the nanoparticles is analyzed. The particle size distribution data generated from DLS is (Figure 16).

Table 5 Values of input parameters and Output values for different experiments

	Input Parameters			Output Variables	
Exp. No.	Wavelength (nm)	RPM (Rotation Per Min)	Fluence (J/ cm^2)	Avg. Size (nm)	Weight Difference (mg)
1	355	10	30	212	3.1
2	355	10	40	190	3.3
3	355	10	50	175	5.1
4	355	20	30	304	4.7
5	355	20	40	177	4.9
6	355	20	50	139	6.8
7	355	30	30	305	3.9
8	355	30	40	188	5.9
9	355	30	50	168	7.4

4.3.2 Morphological and Size analysis

1

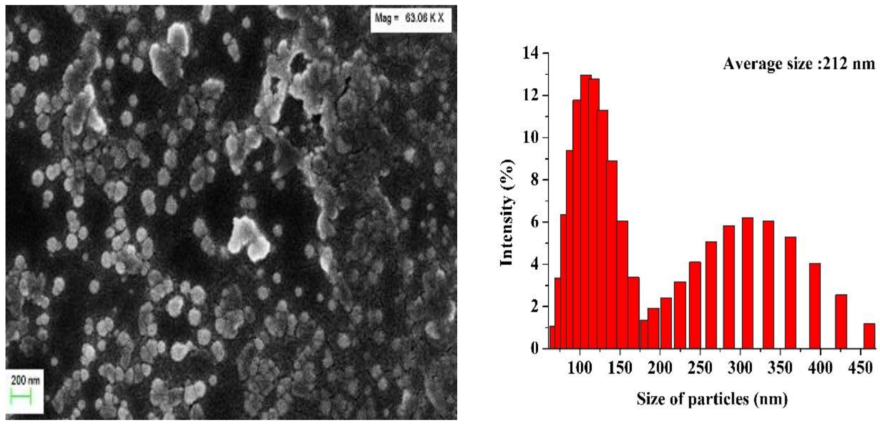

2

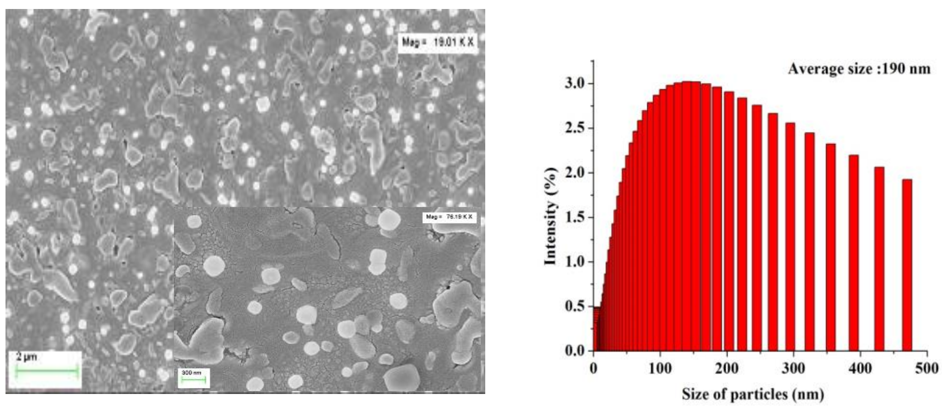

3

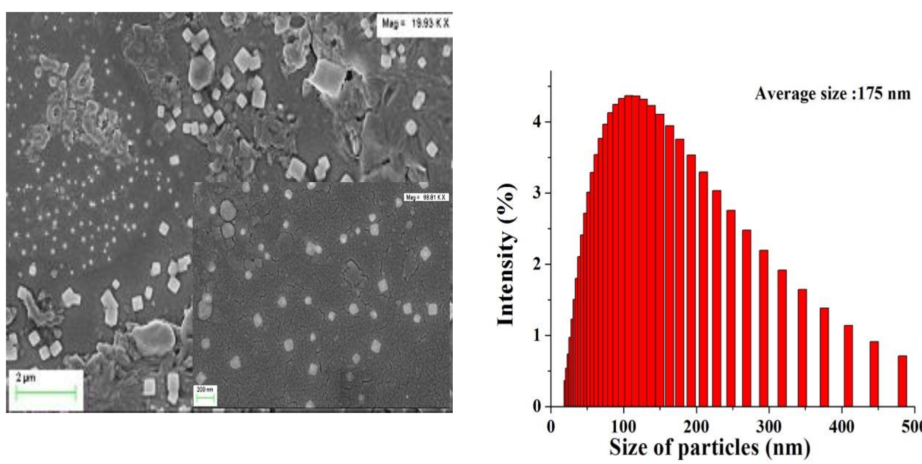

4

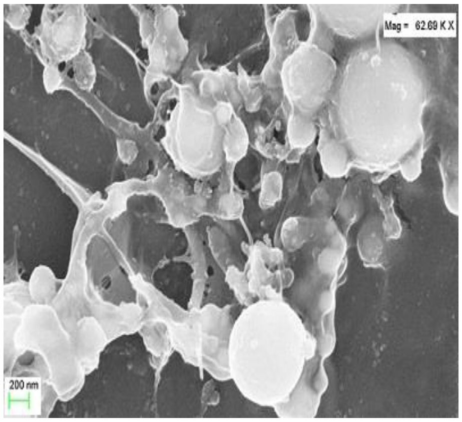

Mag = 62.69 K X
200 nm

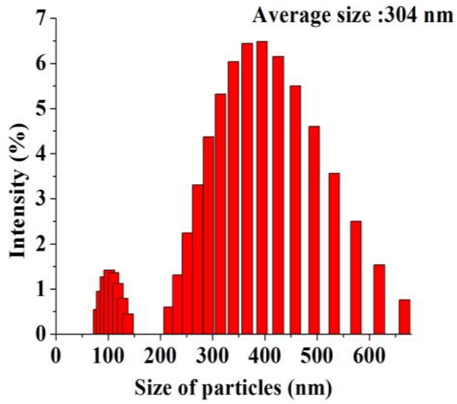

Average size :304 nm
Intensity (%)
Size of particles (nm)

5

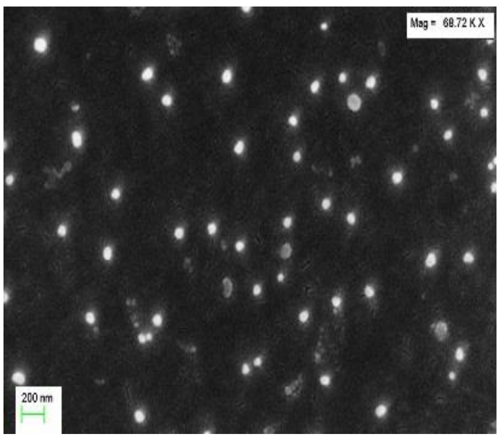

Mag = 69.72 K X
200 nm

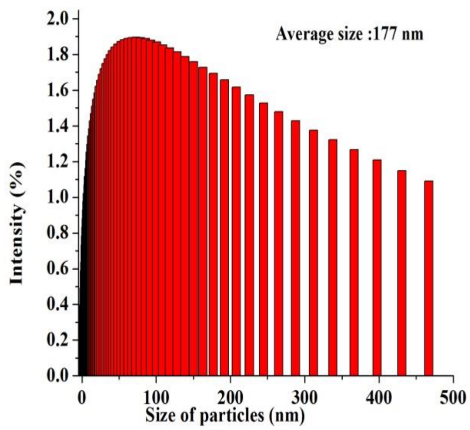

Average size :177 nm
Intensity (%)
Size of particles (nm)

6

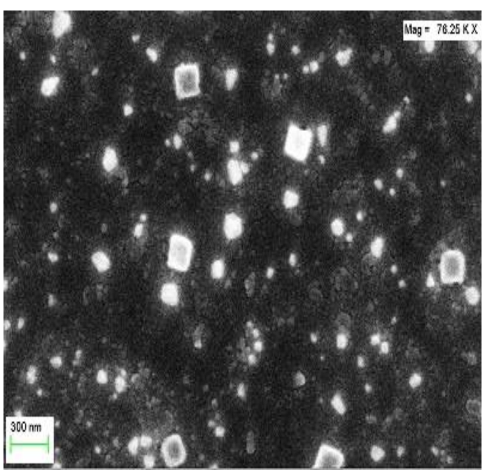

Mag = 76.25 K X
300 nm

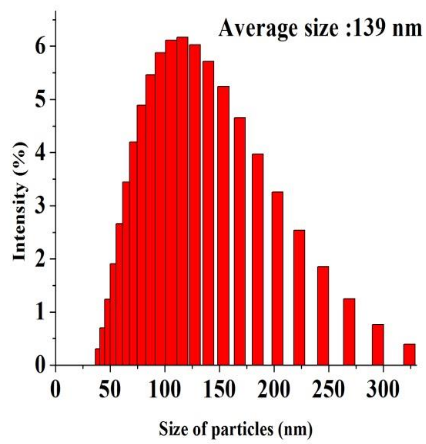

Average size :139 nm
Intensity (%)
Size of particles (nm)

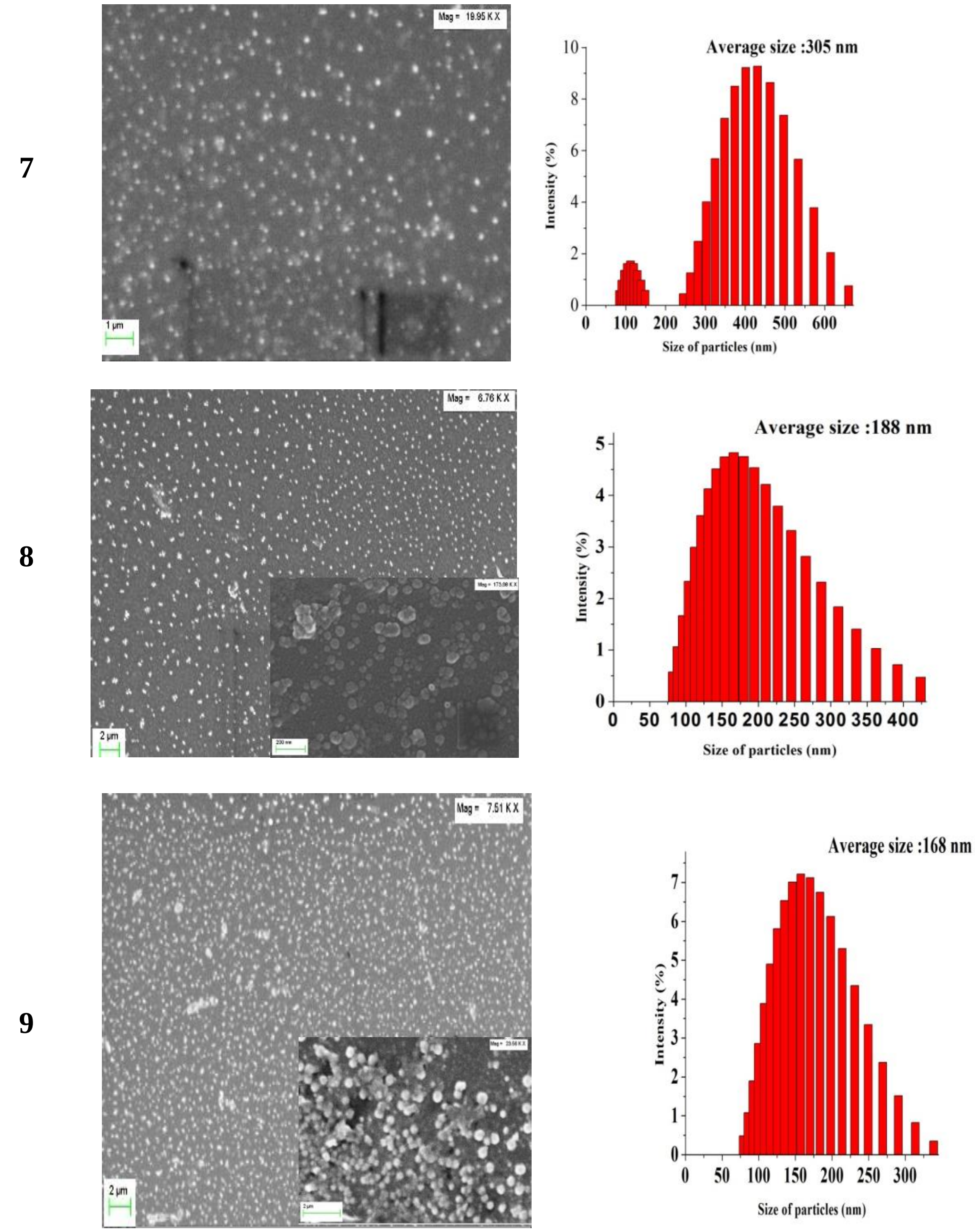

Figure 16 SEM images and corresponding DLS plots (1-9) for different parameters

4.3.3 Influence of laser fluences:

The effect of three different laser fluences (50 J/cm^2, 40 J/cm^2, and 30 J/cm^2) on average size examined from the SEM images at constant RPM. Based on the analysis from Table 5, it was investigated that the average size of nanoparticles were smaller and the formation of nanoparticles increases at higher fluences. Thus it increases the concentration of colloidal solution [22]

During a single laser pulse the nanoparticles are excited due to the absorbance of photons. The light absorption at higher fluence leads to generate smaller size of nanoparticles, however it was observed that the average particle size was less at higher fluences[13]. This might be due to the type of nucleation process during ablation. The direct nucleation of particles acting as growing centres for the incoming species which contribute to varying size distribution[13]

4.3.4 DSC analysis:

The phase transformations temperatures were determined using Netzsch-DSC214 Polyma at a heating rate of 10^{o}C/min with constant flow nitrogen atmosphere.

For DSC analysis we separate out nanoparticles from solution by using Lyophilizer.We used only 0.5 mg nanoparticles so, results as shown in figure 17 is not showing the phase transformation temperature of NiTi NPs. In literature review it was found that when 8.5 mg of NiTi NPs taken for analysis than phase transformation is clearly visible in heating and cooling cycle.

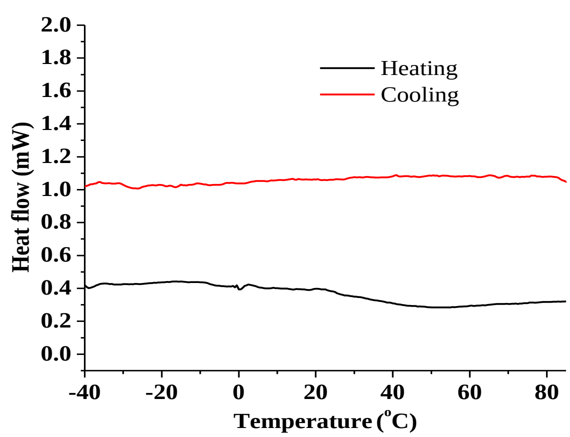

Figure 17 DSC analysis of Nitinanoparticls

4.3.5 Crystallinity and elemental analysis:

Figure 18 shows different structural phases of NiTi at constant laser wavelength and two different fluenc and three different RPM (10, 20, and 30). The crystalline peak of NiTiwas observed for the samples prepared at 355 nm laser wavelength and at fluence of 30 J/cm^2 with different RPM. The additional peak of Ni4Ti3 was observed at 30 RPM. All the nanoparticles synthesized at 355 nm wavelength by varying laser fluences (50 J/cm^2, 40 J/cm^2, and 30 J/cm^2), shows the crystalline peak of NiTi.

The three different phases were observed for all samples attributed to the transformation of NiTi phase to Ni_4Ti_3 intermediate phase and finally Ni_3Ti phase. The probable explanation for transformation of phases might be due to the longer ageing time at equilibrium [23]. It was investigated that the oxide peak was visible from the XRD images as Ti is easily oxidized due to oxygen adsorption [24].

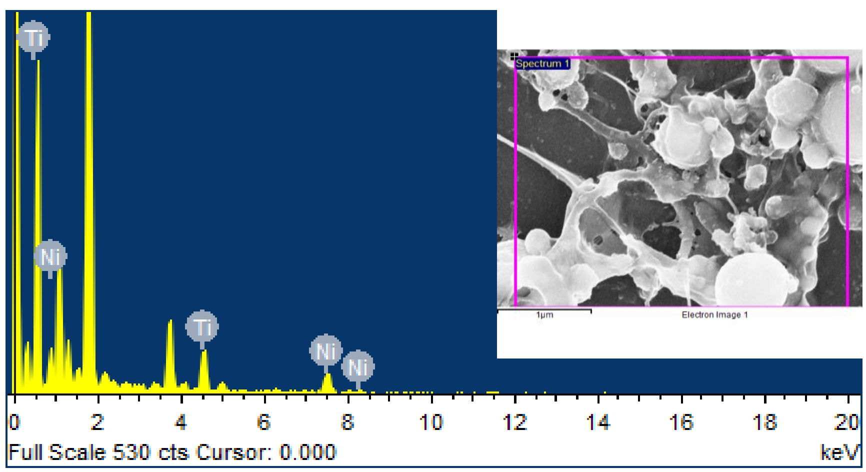

Element	Weight%	Atomic%
Ti K	44.76	49.83
Ni K	55.24	50.17
Totals	100.00	

Figure 18 Shows the composition of NiTi using EDS (Energy Dispersive Microanalysis). This proves the formation of NiTi nanoparticle with the same percentage of element property as the bulk material target.

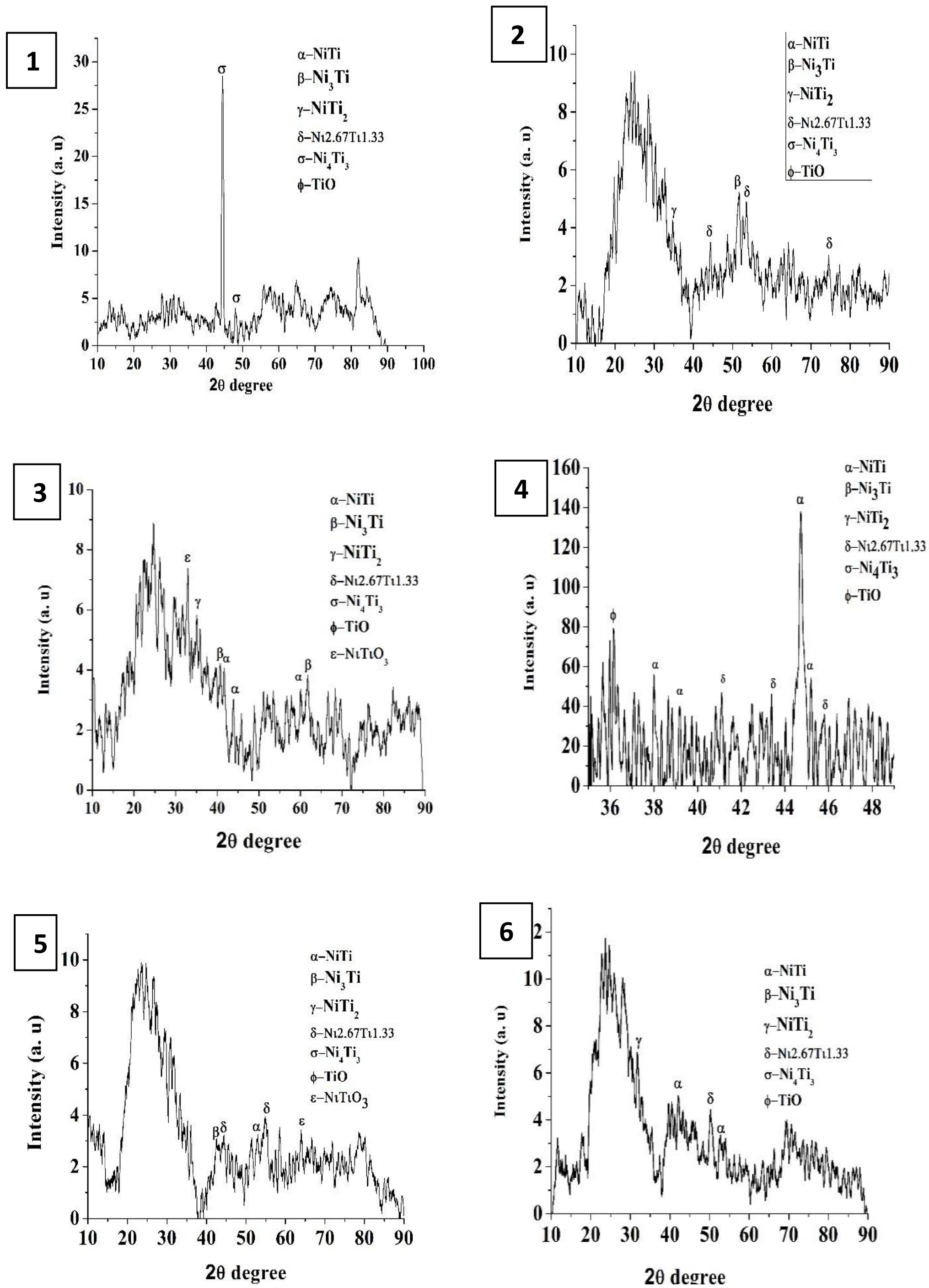
1
Intensity (a. u)
2θ degree
α–NiTi
β–Ni3Ti
γ–NiTi2
δ–Ni2.67Ti1.33
σ–Ni4Ti3
ϕ–TiO
2
Intensity (a. u)
2θ degree
3
Intensity (a. u)
2θ degree
ε–NiTiO3
4
Intensity (a. u)
2θ degree
5
Intensity (a. u)
2θ degree
6
Intensity (a. u)
2θ degree

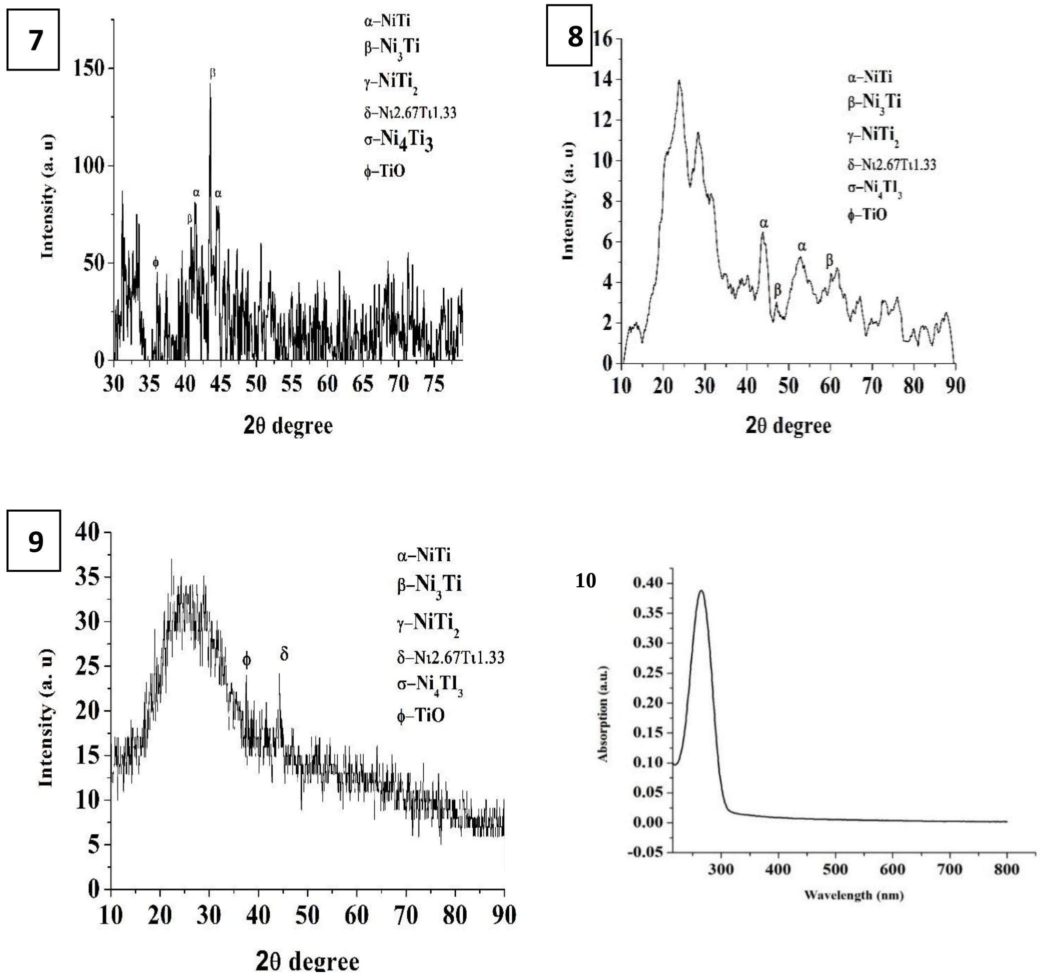

Figure 19 XRD plots (1-9) of nanoparticles for the Different parameters as mention in table and UV-Vis spectra (10).

4.3.7 Influence of absorption co-efficient for nanoparticle formation:

It was observed that the ablation of NiTi target was increasing with increasing the laser fluence. Table 5 shows the amount of ablated target material for 15 min with respect to laser fluencies.NiTi has higher absorption in UV region than visible and IR region of light. It was also observed that the laser ablation efficiency (table 5) was increasing with increasing the rotational speed of the target

Chapter 5 Conclusion and Scope for Future Work

This chapter summarizes the significant achievements and conclusions from the present work highlighting the extent to which the aims and objectives are met. It also presents the possibilities for future work based on the outcomes of the research.

5.1 Conclusions

Liquid assisted laser ablation is a convenient way to generate metal alloy nanoparticles. Laser wavelengths and fluences have an important role incontrolling the size of the nano-particle. Influences of laser parameters like laser wavelength, laser fluence, and speed of rotating metal target have been studied. Effect of different solution like Aceton, Isopropyl alcohol, Methanol, Ethanol and Surfactant Trisodium Citrate Dihydrate also studied.

Following conclusion can be drawn from the present research work:

1. Increase in laser wavelength results in bigger particles size whereas increase in laser fluence form smaller sizes of particles.

2. For NiTi minimum average particle size of 139 nm was observed for the laser wavelength of 355 nm with fluence of 50J/cm^2 at 20 RPM.

3. For Al minimum average particle size of 140 nm was observed for the laser wavelength 355 nm with fluenceof 50J/cm^2 at 10 RPM.

4. The XRD plots at different wavelengths,fluencies and rotationl speed had shown the crystalline peaks of .

5. Alloy form of NiTi and Cu-Al were observed from XRD and EDX images.

6. It was investigated that the formation efficiency of nano-particles was more at higher fluencies and higher RPM.

7. Based on UV–Vis spectroscopy, the optical absorption capacity of Al, Cu-Al and NiTi nanoparticles was high in ultra-violet region than in visible and IR region.

8.It was observed that minimum range of NiTi nanoparticles was 10-20 nm obtains with higher range of particles.

5.2 Scope for the Future Work

1. Fully automation work possible to enable the variations in the parameters.
2. Using Acetone and surfactant solution, we may get the minimum range with more uniform distribution and longer dispersion NPs with the same technique.
3. Temperature control morphological analysis may be possible.
4. Study the mechanical properties of NiTi at nanoscale.
5. Using centrifuge, desired range of NPs separated out from colloidal solution of NPs.

Chapter 6 Bibliography

[1] K. Otsuka and X. Ren, "Physical metallurgy of Ti-Ni-based shape memory alloys," *Prog. Mater. Sci.*, vol. 50, no. 5, pp. 511–678, 2005.

[2] H. R. Ghorbani, "A Review of Methods for Synthesis of Al Nanoparticles," 2014.

[3] T. L. Temple and D. M. Bagnall, "Optical properties of gold and aluminium nanoparticles for silicon solar cell applications," *J. Appl. Phys.*, vol. 109, no. 8, 2011.

[4] D. Zhang, X. Yang, X. Hong, Y. Liu, and J. Feng, "Aluminum nanoparticles enhanced light absorption in silicon solar cell by surface plasmon resonance," *Opt. Quantum Electron.*, no. 99, pp. 1421–1427, 2014.

[5] A. Krishnan, S. Das, S. R. Krishna, and M. Z. A. Khan, "Multilayer nanoparticle arrays for broad spectrum absorption enhancement in thin film solar cells," *Opt. Express*, vol. 22, no. S3, p. A800, 2014.

[6] P. Mandal and S. Sharma, "Progress in plasmonic solar cell efficiency improvement: A status review," *Renew. Sustain. Energy Rev.*, vol. 65, no. November 2016, pp. 537–552, 2016.

[7] S. Pillai, K. R. Catchpole, T. Trupke, and M. A. Green, "Surface plasmon enhanced silicon solar cells," *J. Appl. Phys.*, vol. 101, no. 9, 2007.

[8] T. L. Temple and D. M. Bagnall, "Optical properties of gold and aluminium nanoparticles for silicon solar cell applications," *J. Appl. Phys.*, vol. 109, no. 8, pp. 1–13, 2011.

[9] E. L. Lim, C. C. Yap, M. A. Mat Teridi, C. H. Teh, A. R. bin Mohd Yusoff, and M. H. Hj Jumali, "A review of recent plasmonic nanoparticles incorporated P3HT: PCBM organic thin film solar cells," *Org. Electron.*, vol. 36, pp. 12–28, 2016.

[10] X. Chen, B. Jia, Y. Zhang, and M. Gu, "Exceeding the limit of plasmonic light trapping in textured screen-printed solar cells using Al nanoparticles

and wrinkle-like graphene sheets," *Light Sci. Appl.*, vol. 2, no. 8, p. e92, 2013.

[11] A. BALADI and R. S. MAMOORY, "EFFECT OF LASER WAVELENGTH AND ABLATION TIME ON PULSED LASER ABLATION SYNTHESIS OF AL NANOPARTICLES IN ETHANOL," *Int. J. Mod. Phys. Conf. Ser.*, vol. 05, pp. 58–65, 2012.

[12] M. Ullmann, S. Friedlander, and A. Schmidt-Ott, "Nanoparticle Formation by Laser Ablation," *J. Nanoparticle Res.*, vol. 4, no. 6, pp. 499–509, 2002.

[13] T. Tsuji, K. Iryo, N. Watanabe, and M. Tsuji, "Preparation of silver nanoparticles by laser ablation in solution: Influence of laser wavelength on particle size," *Appl. Surf. Sci.*, vol. 202, no. 1–2, pp. 80–85, 2002.

[14] S. L. Wu, P. K. Chu, X. M. Liu, C. Y. Chung, J. P. Y. Ho, C. L. Chu, S. C. Tjong, K. W. K. Yeung, W. W. Lu, K. M. C. Cheung, and K. D. K. Luk, "Surface characteristics, mechanical properties, and cytocompatibility of oxygen plasma-implanted porous nickel titanium shape memory alloy," *J. Biomed. Mater. Res. - Part A*, vol. 79, no. 1, pp. 139–146, 2006.

[15] S. Z. Mortazavi, P. Parvin, A. Reyhani, A. N. Golikand, and S. Mirershadi, "Effect of laser wavelength at IR (1064 nm) and UV (193 nm) on the structural formation of palladium nanoparticles in deionized water," *J. Phys. Chem. C*, vol. 115, no. 12, pp. 5049–5057, 2011.

[16] S. Barcikowski, A. Hahn, A. V. Kabashin, and B. N. Chichkov, "Properties of nanoparticles generated during femtosecond laser machining in air and water," *Appl. Phys. A Mater. Sci. Process.*, vol. 87, no. 1, pp. 47–55, 2007.

[17] M. Chakif, A. Essaidi, E. Gurevich, A. Ostendorf, O. Prymak, and M. Epple, "Generation of NiTi nanoparticles by femtosecond laser ablation in liquid," *J. Mater. Eng. Perform.*, vol. 23, no. 7, pp. 2482–2486, 2014.

[18] P. Agreement, I. E. Agency, U. States, and T. People, "Introduction 1.1," no. April, pp. 1–8, 2016.

[19] F. U. Processes and E. Storage, *New Materials II*. .

[20] D. O. O. Galindo, "Silver Nanoparticles by Laser Ablation Confined in Alcohol Using an Argon Gas Environment [DOI:

10.2961/jlmn.2016.02.0004],” *J. Laser Micro/Nanoengineering*, vol. 11, no. 2, pp. 158–163, 2016.

[21] A. Hahn, “Influences on Nanoparticle Production during Pulsed Laser Ablation,” *J. Laser Micro/Nanoengineering*, vol. 3, no. 2, pp. 73–77, 2008.

[22] H. Imam, K. Elsayed, M. a Ahmed, and R. Ramdan, “Effect of Experimental Parameters on the Fabrication of Gold Nanoparticles via Laser Ablation,” vol. 2012, no. June, pp. 73–84, 2012.

[23] X. Wang, “Crystallization and Martensitic Transformation Behavior of NiTi Shape Memory Alloy Thin Films,” no. May, p. 128, 2007.

[24] G. Lu, S. L. Bernasek, and J. Schwartz, “Oxidation of a polycrystalline titanium surface by oxygen and water,” *Surf. Sci.*, vol. 458, no. 1, pp. 80–90, 2000.